POCOP–Type Pincer Complexes of Nickel: Synthesis, Characterization, and Ligand Exchange Reactivities of New Cationic Acetonitrile Adducts

ARTICLE *in* ORGANOMETALLICS · JULY 2015

Impact Factor: 4.13 · DOI: 10.1021/acs.organomet.5b00272

3 AUTHORS:

Sébastien Lapointe
Okinawa Institute of Science and Technology
1 PUBLICATION **2** CITATIONS
SEE PROFILE

Boris Vabre
The University of Calgary
16 PUBLICATIONS **121** CITATIONS
SEE PROFILE

Davit Zargarian
Université de Montréal
107 PUBLICATIONS **2,140** CITATIONS
SEE PROFILE

ORGANOMETALLICS

Article

pubs.acs.org/Organometallics

POCOP-Type Pincer Complexes of Nickel: Synthesis, Characterization, and Ligand Exchange Reactivities of New Cationic Acetonitrile Adducts

Sébastien Lapointe, Boris Vabre,[†] and Davit Zargarian*

Département de Chimie, Université de Montréal, Montréal, Québec, Canada H3C 3J7

Supporting Information

ABSTRACT: This report describes the synthesis, characterization, and ligand exchange studies of a family of cationic acetonitrile adducts of nickel featuring resorcinol-based, pincer-type POCOP ligands. The compounds $[(\text{R-POCOP}^{R'})\text{Ni(NCMe)}][OSO_2CF_3]$ (R-POCOP$^{R'}$ = 2,6-$(R'_2PO)_2(R_nC_6H_{3-n})$; R′ = *i*-Pr: R = H (**1**), *p*-Me (**2**), *p*-OMe (**3**), *p*-CO_2Me (**4**), *p*-Br (**5**), *m*,*m*-*t*-Bu_2 (**6**), *m*-OMe (**7**), *m*-CO_2Me (**8**); R′ = *t*-Bu: R = H (**9**), *p*-CO_2Me (**10**)) were prepared in 80−93% yields by reacting the corresponding charge-neutral bromo derivatives with $Ag(OSO_2CF_3)$ in acetonitrile. The impact of the R- and R′-substituents on electronics and structures of **1**−**10** have been probed by NMR, UV−vis, and IR spectra, X-ray crystallography, and cyclic voltammetry measurements. The observed $\nu(C{\equiv}N)$ values were found to increase with the increasing electron-withdrawing nature of R, i.e., in the order **7** < **3** ∼ **2** ∼ **6** < **1** < **5** ∼ **8** < **4** and **9** < **10**. This trend is consistent with the anticipation that enhanced electrophilicity of the nickel center should result in an increase in net MeCN→Ni σ-donation. That this transfer of electron density from acetonitrile to the nickel center does not adequately counteract the impact of electron-withdrawing substituents was evident from the measured redox potentials: the MeO_2C-substituted cations showed the highest oxidation potentials. Moreover, all cationic adducts showed greater oxidation potentials compared with their corresponding charge-neutral bromo precursors. Equilibrium studies conducted with selected $[(\text{R-POCOP}^{R'})\text{Ni(NCMe)}][OSO_2CF_3]$ and (R-POCOP$^{R'}$)NiBr (R′ = *i*-Pr) have confirmed facile MeCN/Br exchange between these derivatives and show that the cationic adducts are stabilized with MeO-POCOP, whereas the charge-neutral bromo species are stabilized with MeO_2C-POCOP. The potential implications of these findings for the catalytic reactivities of the title cationic complexes have been discussed.

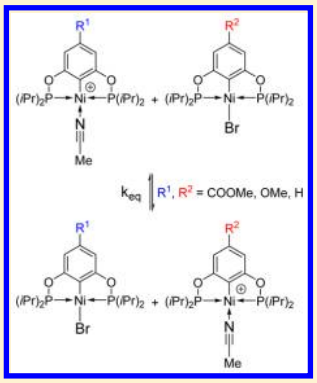

INTRODUCTION

The pioneering studies begun in the 1970s by groups of Shaw[1] and van Koten[2] laid the foundation for what later came to be known as pincer chemistry.[3] Over the nearly four decades since, researchers have combined old and new ligand types with various d- and p-block elements to synthesize numerous pincer complexes and explore their reactivities and physical properties. These developments have been captured in a number of authoritative review articles.[4]

Nickel complexes were among the early pincer derivatives introduced by Shaw and van Koten, but it was only over the past decade that organonickel pincer chemistry experienced major developments. The introduction of many different families of pincer nickel complexes (PCP,[5] $POC_{sp2}OP$,[6] $POC_{sp3}OP$,[7] POCN,[8] PNP,[9] NNN,[10] etc.[11]) has led to exciting developments that have been reviewed recently.[4e,12] Among these, resorcinol-based POCOP-Ni systems have proven particularly popular due to the facile synthesis of variously substituted ligands and their complexes (via C−H nickelation),[6b,d,7a,13] as well as the interesting catalytic transformations these compounds promote.[14]

We have initiated a systematic study aimed at mapping out the impact of differently substituted, resorcinol-derived POCOP ligands on structures and electronic properties of their cationic Ni-acetonitrile adducts. Thus, we have reported on the influence of *P*- and aromatic ring substituents on C−H nickelation rates, structures, and redox potentials of charge-neutral complexes (R-POCOP$^{R'}$)NiBr.[15] Analogous studies have been reported by other groups on POCOP complexes of Ir and Pt.[16] These reports have inspired us to study the impact of *P*- and aromatic ring substituents on the structures and electronic properties of cationic adducts featuring POCOP ligands. Reported herein are the syntheses, and spectroscopic and structural studies, redox potential measurements, and ligand exchange reactivities of the cationic acetonitrile adducts $[(\text{R-POCOP}^{R'})\text{Ni(NCMe)}][OSO_2CF_3]$, where R and R′ represent, respectively, various substituents on the resorcinol aromatic ring (H, *p*-Me, *p*-OMe, *p*-CO_2Me, *p*-Br, *m*-OMe, *m*-CO_2Me, *m*,*m*-*t*-Bu_2) and *P*-substituents (*i*-Pr, *t*-Bu). Given the importance of this family of complexes in a number of

Received: April 6, 2015
Published: July 10, 2015

DOI: 10.1021/acs.organomet.5b00272
Organometallics 2015, 34, 3520−3531

interesting catalytic reactivities,[7a,14c,17] we hope that the results of our study will provide a basis for tuning the reactivities of [(R-POCOP$^{R'}$)Ni(L)][OSO_2CF_3] for different catalytic applications.

RESULTS AND DISCUSSION

Synthesis of [(R-POCOP$^{R'}$)Ni(NCMe)][OSO_2CF_3]. The target cationic complexes were prepared by treating the charge-neutral bromo derivatives (R-POCOP$^{R'}$)NiBr with 1.2 equiv of AgOTf in dry acetonitrile under nitrogen and in the absence of light (Scheme 1). The charge-neutral bromide precursors used in these syntheses were, in turn, obtained from the rt reaction of the preligands R-POC^{H}OP with $NiBr_2(NCMe)_2$ in the presence of 1.2 equiv of NEt_3. It should be noted that all but one of these precursors are known species that have been reported previously;[15a] the only new bromide derivative, (*p*-Br-POCOP$^{R'}$)NiBr (R′ = *i*Pr, **5′**), was prepared in the same manner as its counterparts **1′**−**4′** using the new preligand *p*-Br-POC^{H}OP$^{i\text{-}Pr}$. The latter was prepared by phosphorylation of 5-bromoresorcinol (Scheme 1), which was itself obtained from acidic hydrolysis of 3,5-dimethoxybromobenzene using a modified literature procedure.[18]

Scheme 1. General Synthetic Scheme for Complexes 1−10

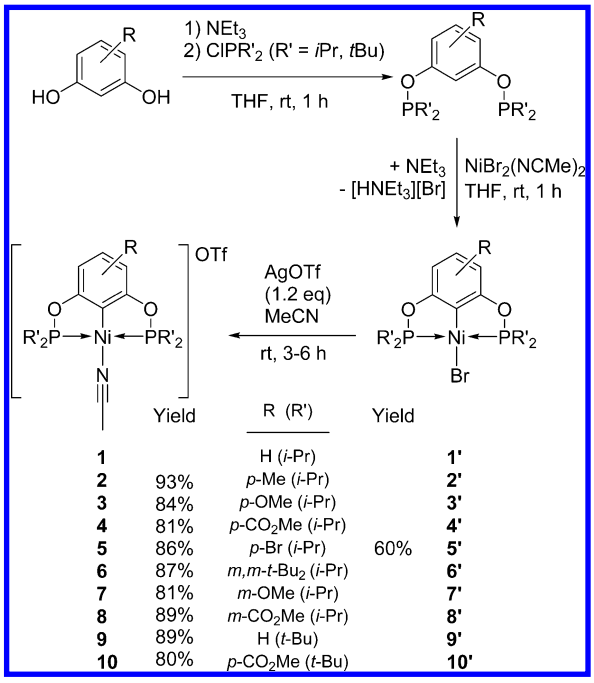

The workup procedure for the cationic complexes consisted of cannula filtration of the final reaction mixture, followed by a second filtration through a short Celite plug to remove AgBr and furnish the target complexes as yellow powders in 80−93% yields. These cationic adducts proved to be less stable than their bromo precursors: storing analytically pure samples in the drybox (without protection from ambient light) led to a gradual color change from yellow to dark green. Eluting a CH_2Cl_2 suspension of these postdecomposition green solids through a short Celite column left a black residue on top of the column and furnished the desired cationic complexes in analytically pure form. Storing the purified samples under inert atmosphere inside a −37 °C freezer circumvented further decomposition.

The title cationic adducts as well as the new bromo derivative **5′** were characterized by spectroscopy (NMR, IR, and UV−vis) and cyclic voltammetry. Single-crystal X-ray diffraction studies were also carried out for complexes **5′**, **2**−**6**, **9**, and **10**; single crystals suitable for diffraction studies could not be obtained for complexes **7** and **8**, whereas the solid-state structure of the parent cation **1** has been reported previously.[13] The solid-state structures are discussed below, followed by the results of the spectroscopic studies and electrochemical analyses.

Solid-State Structures. Table 1 lists the most pertinent structural parameters for the complexes that were subjected to X-ray diffraction studies, and Figures 1−3 show a side view of the molecular diagrams of adducts **4**, **6**, and **10**; the molecular diagrams for the remaining four complexes, the front view of the molecular diagrams of complexes **4**, **6**, and **10**, and the details of the diffraction studies are given in Figures S1−S8 and Tables S1 and S2 (see the Supporting Information, SI).

The nickel center in all complexes adopts a square planar geometry that displays slight distortions due, primarily, to the small bite angle of the POCOP ligands: P−Ni−P ≈ 163−165°.

Table 1. Selected Bond Distances (Å) and Angles (deg) for Cationic Adducts 1−10 and Charge-Neutral Complexes 1′−10′

complex	Ni−C	Ni−N/Br	N≡C	Ni−P_1	Ni−P_2	P_1−Ni−P_2	C−Ni−N/Br
1[a]	1.881(2)	1.874(2)	1.140(3)	2.1683(7)	2.1704(7)	164.38(3)	175.8(1)
2	1.879(3)	1.875(2)	1.142(4)	2.1693(8)	2.1687(7)	163.52(3)	171.7(1)
3	1.884(2)	1.881(2)	1.135(3)	2.1784(5)	2.1747(5)	163.16(2)	176.84(7)
4	1.880(2)	1.879(2)	1.138(2)	2.1698(4)	2.1748(4)	164.45(1)	178.43(6)
5	1.879(3)	1.871(3)	1.145(4)	2.1685(9)	2.171(2)	164.44(4)	176.6(2)
6	1.890(2)	1.875(2)	1.140(2)	2.1785(5)	2.1640(4)	163.79(2)	170.35(6)
9	1.885(2)	1.879(2)	1.140(2)	2.1944(5)	2.1946(5)	163.57(2)	179.02(6)
10	1.881(2)	1.876(2)	1.146(2)	2.1933(4)	2.1922(4)	164.025(1)	178.51(6)
1′[a]	1.885(3)	2.3231(5)		2.1534(8)	2.1422(8)	164.92(4)	178.10(8)
2′[a]	1.882(3)	2.3305(5)		2.1584(4)	2.1584(4)	164.21(3)	180.0(1)
3′[a]	1.877(2)	2.319(1)		2.155(1)	2.152(1)	164.65(2)	178.25(6)
4′[a]	1.872(2)	2.312(1)		2.157(1)	2.159(1)	165.26(2)	179.3(1)
5′	1.877(2)	2.3211(5)		2.1500(7)	2.1467(8)	163.89(3)	178.74(8)
6′[a]	1.892(4)	2.320(1)		2.139(1)	2.143(1)	165.06(5)	179.08(12)
9′[a]	1.887(2)	2.338(2)		2.193(1)	2.189(1)	164.13(3)	179.7(1)
10′[a]	1.877(2)	2.321(1)		2.189(1)	2.194(1)	164.58(3)	178.25(7)

[a]Previously reported complexes.[13,15a]

DOI: 10.1021/acs.organomet.5b00272
Organometallics 2015, 34, 3520−3531

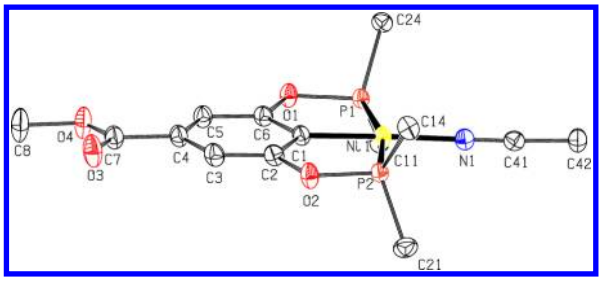

Figure 1. Molecular diagram for complex **4**. Thermal ellipsoids are shown at the 50% probability level. Hydrogens and the *P*-substituents have been removed from this diagram for clarity.

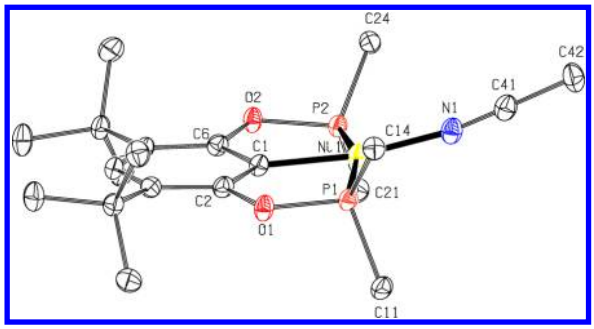

Figure 2. Molecular diagram for complex **6**. Thermal ellipsoids are shown at the 50% probability level. Hydrogens and the *P*-substituents have been removed from this diagram for clarity.

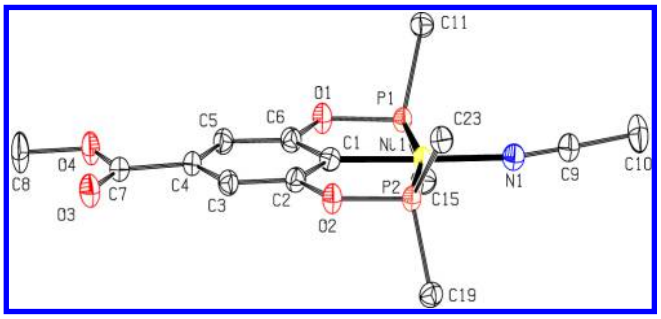

Figure 3. Molecular diagram for complex **10**. Thermal ellipsoids are shown at the 50% probability level. Hydrogens and the *P*-substituents have been removed from this diagram for clarity.

The displacement of the nickel atom out of the coordination plane (P_1–N–P_2–C_{ipso}) is either negligible (<0.01 Å) or very minor (0.02–0.05 Å). Another source of notable structural distortion is the C_{ipso}–Ni–N angle, which is more acute in some cases due to the lifting of the acetonitrile moiety out of the coordination plane. For instance, C_{ipso}–Ni–N angles of ca. 170–172° were found in complexes **2** (R = *p*-Me) and **6** (R = *m*,*m*-*t*-Bu_2), in contrast to angles of 175–180° in the remainder of the complexes; thus, it is difficult to establish with confidence whether these deviations are due to steric or electronic factors.

The Ni–P distances show some variations in these compounds. First, the *t*-Bu_2P–Ni distances are much longer than their *i*-Pr_2P–Ni counterparts, particularly for the charge-neutral bromo derivatives: average of 2.19 Å for *t*-Bu_2P complexes vs 2.15 Å for *i*-Pr_2P complexes. Moreover, the cationic adducts display consistently longer Ni–P distances relative to their charge-neutral bromo counterparts, particularly among the *i*-Pr_2P derivatives: average of 2.17 vs 2.15 Å, respectively. Finally, the aromatic ring substituent(s) R appear to have some impact on the *i*-Pr_2P–Ni distances (range = 2.139–2.158 Å), whereas this impact is more muted in the cationic adducts (range = 2.168–2.179 Å). The smallest Ni–P distances (ca. 2.14 Å) were found in the bromo complex **6′**, featuring the *m*,*m*-(*t*-Bu)$_2$ substituents; this observation was made previously and has been interpreted elsewhere.[15a] Additional bond distances and angles for cationic adducts reported in Table 1 can be found in Table S3 in the SI.

Most of the remaining Ni–X distances appear to be insensitive to the nature of the ring substituents. Thus, the Ni–C_{ipso} distances are essentially equal in all structures, whether cationic adducts or charge-neutral bromides (1.87–1.89 Å). Quite uniform distances were also observed for Ni–N (1.87–1.88 Å) and Ni–Br (2.31–2.34 Å) bonds. The observed Ni–N and N≡C distances fall closer to the lower values in the range of distances available in the Cambridge Structural Database: ca. 1.88 vs 1.71–2.51 Å for Ni–N and 1.14 vs 0.91–1.69 Å for N≡C. The Ni–O distances of 3.9–5.4 Å are very long compared to the corresponding distances in complexes wherein the triflate anion is directly bound to the Ni(II) center (average of 2.05 Å);[19] we conclude that little or no covalent Ni–OSO_2CF_3 interactions are present in our cationic acetonitrile adducts.

IR Analyses. The IR spectra recorded using solid samples of the cationic complexes showed the characteristic bands for ν(C≡N) (ca. 2329–2293 cm^{-1}), ν(SO) (ca. 1270, 1030, and 636 cm^{-1}), and ν(CF) (ca. 1135 cm^{-1}) (see Table S4 in the SI). Comparing the ν(C≡N) values in various complexes shows a fairly clear correlation between the electronic nature of ring substituents R and the C–N bond strength (Table 2). For instance, replacing the H at the *para* position of the central ring (with respect to the metalated *i*-C) by the electron-withdrawing substituent CO_2Me increases the ν(C≡N) values by 32 cm^{-1} (**1** vs **4**) or 22 cm^{-1} (**9** vs **10**). The frequency shift, $\Delta\nu$(C≡N), observed on going from **1** to **5** was +5 cm^{-1}, which shows that the impact of Br is smaller in magnitude but in the same direction as that of CO_2Me.

In the case of adducts bearing the electron-releasing substituents *p*-Me and *p*-OMe, the impact on ν(C≡N) was similarly small in magnitude but in the opposite direction: $\Delta\nu$(C≡N) = −3 cm^{-1} in **2** and −4 cm^{-1} in **3**. Moreover, the same types of frequency shifts result from substitution at the *m*-position, but in this case the electron-releasing substituent OMe leads to a larger impact than its electron-withdrawing counterpart CO_2Me: $\Delta\nu$(C≡N) = −13 cm^{-1} in **7** and +6 cm^{-1} in **8**. Finally, the fairly small impact of the two *t*-Bu substituents in adduct **6** ($\Delta\nu$(C≡N) = −3 cm^{-1}) should be interpreted more cautiously, because it likely is a composite of the steric and electronic effects of these substituents.[20]

The observed correlation between ν(C≡N) values and the POCOP ring substituents R can be rationalized in terms of the MO description of bonding in acetonitrile, as follows. Similarly to CO, acetonitrile's HOMO possesses a certain degree of antibonding character with respect to the C≡N bond, such that σ-donation from this HOMO to a Ni-based acceptor orbital should reinforce the C–N bond and increase the value of ν(C≡N).[22] This phenomenon is underlined by the observation that in all the acetonitrile adducts the C≡N stretching frequency is much higher than that of free acetonitrile (2252 cm^{-1}), consistent with a net transfer of charge from acetonitrile to the Ni center.

It follows then that ν(C≡N) values in the adducts examined here should reflect the approximate electron-donating character of R-POCOP ligands, those with electron-withdrawing

DOI: 10.1021/acs.organomet.5b00272
Organometallics 2015, 34, 3520–3531

Table 2. ν(C≡N) Data for 1−10, Related Complexes, and Free MeCN

complex	ν(C≡N) (cm^{-1})	$\Delta\nu$(C≡N) (cm^{-1})[c]
[(H-POCOP$^{i\text{-}Pr}$)Ni(NCMe)][OSO_2CF_3], **1**[a]	2297 (2292)[b]	45 (40)[b]
[(*p*-Me-POCOP$^{i\text{-}Pr}$)Ni(NCMe)][OSO_2CF_3], **2**	2294	42
[(*p*-OMe-POCOP$^{i\text{-}Pr}$)Ni(NCMe)][OSO_2CF_3], **3**	2293	41
[(*p*-CO_2Me-POCOP$^{i\text{-}Pr}$)Ni(NCMe)][OSO_2CF_3], **4**	2329	77
[(*p*-Br-POCOP$^{i\text{-}Pr}$)Ni(NCMe)][OSO_2CF_3], **5**	2302	50
[(*m*,*m*-*t*-Bu_2-POCOP$^{i\text{-}Pr}$)Ni(NCMe)][OSO_2CF_3], **6**	2294	42
[(*m*-OMe-POCOP$^{i\text{-}Pr}$)Ni(NCMe)][OSO_2CF_3], **7**	2284	32
[(*m*-CO_2Me-POCOP$^{i\text{-}Pr}$)Ni(NCMe)][OSO_2CF_3], **8**	2303	51
[(H-POCOP$^{t\text{-}Bu}$)Ni(NCMe)][OSO_2CF_3], **9**	2293	41
[(*p*-CO_2Me-POCOP$^{t\text{-}Bu}$)Ni(NCMe)][OSO_2CF_3], **10**	2315	63
[(H-$POC_{sp3}OP^{i\text{-}Pr}$)Ni(NCMe)][$OSO_2CF_3$][a]	2284	32
[(H-PCP$^{i\text{-}Pr}$)Ni(NCMe)][BPh_4][a]	2282	30
[(H-$PC_{sp3}P^{i\text{-}Pr}$)Ni(NCMe)][BPh_4][a]	2274	22
[(H-POCOP^{Ph})Ni(NCMe)][OSO_2CF_3][a]	2297	45
[(H-POCOP$^{i\text{-}Pr}$)Ni(NCCH=CH_2)][OSO_2CF_3][a]	2257	
[(H-$POC_{sp3}OP^{i\text{-}Pr}$)Ni(NCCH=$CH_2$)][$OSO_2CF_3$][a]	2252	

[a]Previously reported complexes.[13,14b,c,21b] [b]For complex **1**, the ν(CN) values in parentheses were measured using KBr pellets to provide a comparison to the solid-state ATR measurements used in the discussion. [c]$\Delta\nu$(CN) is relative to the free MeCN stretching frequency (2252 cm^{-1}) measured under our experimental conditions.

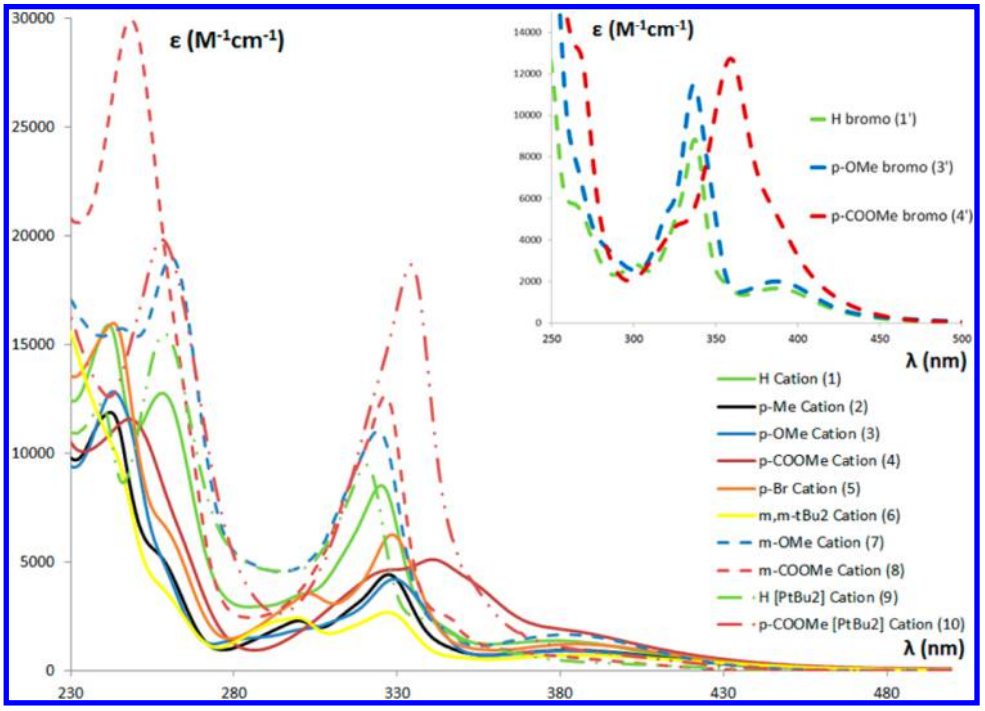

Figure 4. UV−vis spectra of cationic complexes **1**−**10** in full, dashed, and "dash dot dot" lines and of complexes **1**′, **3**′, and **4**′ in dashed lines for comparison. The spectra were recorded in air, using 10^{-4} M CH_2Cl_2 solutions.

substituents allowing greater MeCN→Ni donation and showing higher ν(C≡N) values, and vice versa. This is reflected in plots of the ν(C≡N) stretching frequencies for complexes **1**−**10** and the σ_m or σ_p Hammett coefficients for the corresponding ring substituents R (Figures S9−S11 in the SI). Moreover, it stands to reason that the degree of electron donation from RCN to the electrophilic Ni center should be fairly proportional to its degree of activation toward nucleophiles. Hence, ν(C≡N) values can help estimate the degree of nitrile activation toward outer-sphere nucleophilic attacks either at the nitrile carbon, as in amidination,[17,23] or at the R moiety, as in Michael-type hydroamination of acrylonitrile and its substituted derivatives.[13,14b,c,24]

The above arguments can be extended to other structural parameters in [(pincer)Ni(NCR)]$^+$ and their impact on ν(C≡N) values. For instance, changing the ligand backbone from an aromatic to an aliphatic skeleton has a significant effect on ν(C≡N), as seen from the values for **1** (2297 cm^{-1}) and its $POC_{sp3}OP$ counterpart [(H-$POC_{sp3}OP^{iPr}$)Ni(NCMe)]$^-$[OSO_2CF_3] (2284 cm^{-1}).[13] A similar influence is exerted by the nature of the PR'_2 moiety: replacing the phosphinite moiety by a better net donor phosphine moiety (P−O vs P−CH_2 connections) leads to a significant decrease in ν(C≡N) values from 2297 cm^{-1} in **1** to 2282 cm^{-1} in its PCP analogue [(H-PCP^{iPr})Ni(NCMe)][BPh_4].[14c] A further decrease in the ν(C≡N) value to 2274 cm^{-1} is observed in the

DOI: 10.1021/acs.organomet.5b00272
Organometallics 2015, 34, 3520−3531

aliphatic $PC_{sp3}P$ analogue $[(H\text{-}PC_{sp3}P)Ni(NCMe)][BPh_4]$.[14c] These observations are consistent with lower net donation from MeCN to Ni ligated by strong donor ligands.

The influence of *P*-substituents R′ on $\nu(C{\equiv}N)$ values can be discerned from a comparison among the following two series of complexes: $[(H\text{-}POCOP^{Ph})Ni(NCMe)][OSO_2CF_3]$[14b] vs $[(H\text{-}POCOP^{i\text{-}Pr})Ni(NCMe)][OSO_2CF_3]$ (**1**) vs $[(H\text{-}POCOP^{t\text{-}Bu})Ni(NCMe)][OSO_2CF_3]$ (**9**); $[(p\text{-}CO_2Me\text{-}POCOP^{i\text{-}Pr})Ni(NCMe)][OCO_2CF_3]$ (**4**) vs $[(p\text{-}CO_2Me\text{-}POCOP^{t\text{-}Bu})Ni(NCMe)][OSO_2CF_3]$ (**10**). This comparison confirms that for both of these series the observed correlation is in line with the anticipated donor strength of the different *P*-substituents, i.e., Ph < *i*-Pr < *t*-Bu for the first series and *i*-Pr < *t*-Bu for the second.[25] On the other hand, the *t*-Bu_2P complexes display the longest Ni−P distances (2.195(1) Å in **9** vs 2.173(1) Å in **1**; 2.1928(8) Å in **10** vs 2.1723(8) Å in **4**), which should normally lead to poorer orbital overlap between the Ni center and the bulky *t*-Bu_2P moiety, less efficient P→Ni donation, and hence more electrophilic Ni centers in **9** and **10**. However, the opposite scenario is implied by the IR data. We have further probed this issue through cyclic voltammetry measurements, and, as will be discussed below, the redox potentials of these complexes tend to contradict the implications of $\nu(C{\equiv}N)$ values for adducts **9** and **10**.

NMR Studies. Table S5 in the SI lists the pertinent ^{31}P, ^{1}H, and ^{13}C NMR data for complexes **1**−**10**, and the relevant spectra are shown in Figures S13−S51 in the SI. The ^{31}P NMR spectra show a rather narrow chemical shift range, ca. 192−196 ppm for **1**−**8** and ca. 198−200 ppm for **9** and **10**, indicating that the ring substituents do not influence ^{31}P δ values significantly. To be sure, the electron-withdrawing substituents CO_2Me and Br seem to lead to downfield ^{31}P chemical shifts relative to the parent complex **1**, but no clear trend is evident with electron-releasing substituents in any of the spectra. The parent compound **1** and its symmetrically substituted analogues **2**−**6**, **9**, and **10** show a singlet, whereas the unsymmetrical complex **7** shows the anticipated doublet of doublets for the two chemically inequivalent ^{31}P nuclei (see Figure S37, SI). Complex **8**, the only other compound in the series bearing an unsymmetrically substituted POCOP ligand, shows a ^{31}P singlet instead of the anticipated AB signals (see Figure S43 in the SI); this is presumably because the difference in the chemical shifts of the two inequivalent ^{31}P nuclei is smaller than the resolution of the spectrum. The ^{13}C NMR spectra of **7** and **8** showed ABX signals for the methyne carbon nuclei, giving an apparent dt for **7** and a partially resolved dd for **8**. (See Figures S38 and S42 in the SI.)

Absorption Spectra. The UV−vis spectra of complexes **1′**−**10′** and **1**−**10** were recorded in dry CH_2Cl_2 (ca. 10^{-4} M solutions). The wavelengths and molar absorptivity of all complexes are tabulated in Table S6 in the SI, and the spectra of complexes **1**−**10**, **1′**, **3′**, and **4′** are shown in Figure 4. The low-energy bands (370−420 nm) display low intensities and appear fairly indifferent to the nature of ring substituents, implying that they are likely spin-allowed but Laporte-forbidden d−d transitions. Conversely, the bands in the 300−350 nm region that are most affected by the nature of the ring substituent likely represent $\pi{\rightarrow}\pi^*$ transitions. For instance, the λ_{max} for complex **4**, bearing the *p*-CO_2Me substituent, is at 341 nm, 12−16 nm higher than those of the unsubstituted complex **1** and the complexes **2** and **3**, bearing electron-releasing substituents. This observation can be rationalized by the fact that electron-withdrawing groups stabilize the charge buildup in the excited state better than would electron-donating groups, thus lowering the $\pi{\rightarrow}\pi^*$ transition energy and leading to a red shift.[15a] In other words, ligands bearing the most effective electron-accepting ring substituent should exhibit lower energy $\pi{\rightarrow}\pi^*$ transitions. A similar phenomenon is at work for the MLCT transition in the complexes. As shown in Figure 4 and Table S6 in the SI, the MLCT transitions of the charge-neutral bromide complexes feature molar absorptivities and wavelengths that are very similar to those of cationic acetonitrile adducts.

Electrochemical Studies. For the cationic adducts under study, another indication of how POCOP ring or *P*-substituents affect the electron density of the Ni center can be extrapolated from their redox potentials. We have conducted cyclic voltammetry measurements on the charge-neutral bromo complexes **1′**−**10′** and the cationic acetonitrile adducts **1**−**10**, and the results are reported in Table 3; the cationic adducts are presented in Figures S52−S63 in the SI. Most complexes displayed irreversible oxidation, whereas complexes **3**, **6**, and **7** displayed quasi-reversible behavior, presumably because the substituents *m,m*-*t*-Bu_2 and *p*- and *m*-OMe stabilize the Ni center sufficiently to prevent decomposition during the $Ni^{II}{\rightarrow}Ni^{III}$ oxidation event. The redox potentials obtained from these measurements (calibrated against the Cp_2Fe/Cp_2Fe^+ redox couple) are listed in Table 3 and plotted against Hammett coefficients for the *para* and *meta* substituents (Figure S64, SI).

Table 3. Redox Potentials of 1−10 and 1′−10′[a]

complex	E_{ox} or $E_{1/2}$ (mV)	complex	E_{ox} or $E_{1/2}$ (mV)
1[b]	1168	**1′**[b]	817
2	1151	**2′**[b]	692
3	933 (922)	**3′**[b]	560 (572)
4	1269	**4′**[b]	776
5	1159	**5′**	738
6	1012 (997)	**6′**[b]	567
7	977 (967)	**7′**[b]	761 (715)
8	1262	**8′**[b]	900
9	1298	**9′**[b]	800 (750)
10	1457	**10′**[b]	920 (860)

[a] $E_{1/2}$ values are given for quasi-reversible redox couples. See caption of Figure 5 for measurement details. [b] Previously reported complexes[13,15a] for which the redox values were remeasured in the current experimental conditions.

The electrochemical measurements reveal the following order of oxidation potential for $[(R\text{-}POCOP^{R'})Ni(NCMe)][OSO_2CF_3]$ as a function of both ring substituent R and *P*-substituent R′: *p*-CO_2Me [*t*-Bu_2P] (**10**) > H [*t*-Bu_2P] (**9**) > *p*-CO_2Me (**4**) > *m*-CO_2Me (**8**) > *p*-Br (**5**) > H (**1**) > *p*-Me (**2**) > *m,m*-*t*-Bu_2 (**6**) > *m*-OMe (**7**) > *p*-OMe (**3**). If we focus on the *i*-Pr_2P complexes, the observed order of oxidation potentials is consistent with the anticipated electronic impact of the aromatic-ring substituents. This trend shows some similarities to the corresponding trend in $\nu(C{\equiv}N)$ stretching frequencies (**4** > **8** > **5** > **1** > **2**), but there are also significant differences. The most striking differences between these two trends lie primarily in the positions of the *t*-Bu_2P-containing complexes **9** and **10**. It is conceivable that the steric bulk of the *t*-Bu_2P moieties constrains the acetonitrile moiety in a configuration that would reduce orbital overlap of the nitrogen atom with the nickel center, thus lowering the $\nu(C{\equiv}N)$ values compared to their *i*-Pr_2P analogues.

DOI: 10.1021/acs.organomet.5b00272
Organometallics 2015, 34, 3520−3531

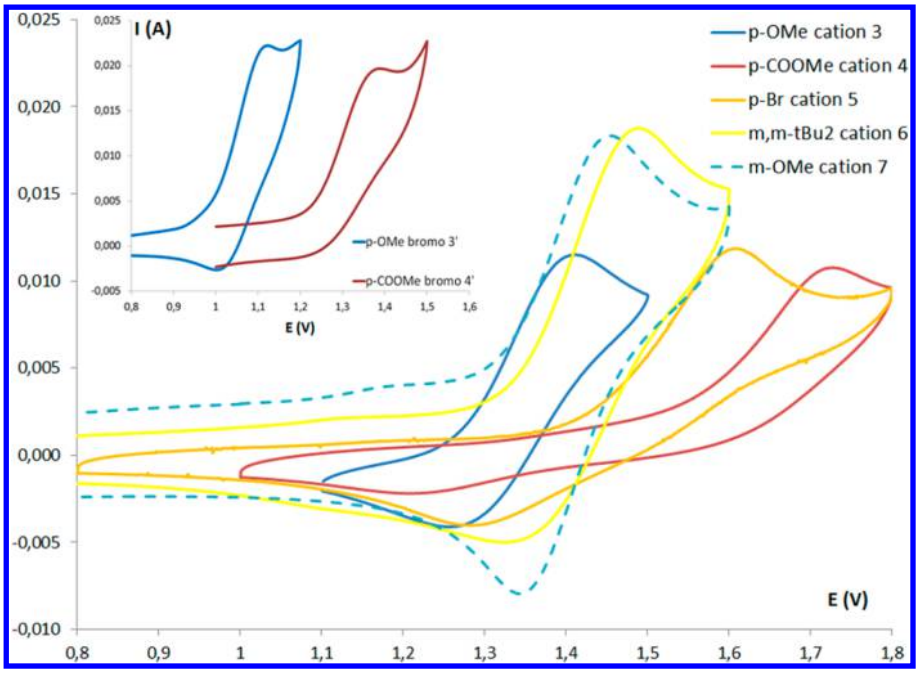

Figure 5. Cyclic voltammograms of **3**−**7**, **3**′, and **4**′. The measurements were carried out at 298 K using dry CH_2Cl_2 solutions containing equimolar quantities of the given complex and $[Bu_4N][PF_6]$ as electrolyte (10^{-4} M). Prior to beginning the measurements, the samples were purged for 2 min by bubbling a stream of N_2, and a nitrogen atmosphere was maintained over the samples throughout the measurements. A scan rate of 100 mV s^{-1} was used, and the potentials were referenced to the Cp_2Fe/Cp_2Fe^+ redox couple.

Another insight provided by the oxidation potentials shown in Table 3 pertains to the impact of *P*-substituents on the electronic density of the metal center: the *t*-Bu_2P analogues **9** and **10** have higher oxidation potentials than their *i*-Pr_2P counterparts, implying that among the cationic acetonitrile adducts the supposedly better donor *t*-Bu substituents seem to decrease instead the electron density on the Ni center. A similar phenomenon has been observed in previous studies and has been attributed to the longer Ni−P distances with the sterically larger *t*-Bu_2P moieties.[5h] Inspection of the Ni−P distances in our complexes supports this assertion: the Ni−P(*t*-Bu)$_2$ bond distance is significantly longer than Ni−P(*i*-Pr)$_2$ in every case for both the cationic adducts and the charge-neutral bromo species. On the other hand, this phenomenon appears to be more complex, because the charge-neutral bromo complexes represent a less clear-cut scenario: complexes **10**′ and **4**′ show the oxidation potential order observed for their cationic analogues, whereas **9**′ and **1**′ show the opposite order. Evidently, more studies are required to develop a better understanding of this phenomenon.

Finally, the overall charge of the complexes seems to be a significant factor in the oxidation potential of the complexes studied here: all cationic adducts are more difficult to oxidize than their neutral bromo counterparts. We note also that oxidation potential trends are maintained regardless of the overall charge. In the *i*-Pr_2P series, for instance, the same oxidation potential trend is seen with the charge-neutral and cationic complexes bearing the following ring substituents: *p*-CO_2Me > *m*-CO_2Me > H > *p*-Me > *m*-OMe > *p*-OMe. The same is also true for the two remaining cases, *p*-Br > *m*,*m*-*t*-Bu_2, as well as for the two *t*-Bu_2P complexes (*p*-CO_2Me > H).

Oxidation Studies with $FeCp_2$. As alluded to above, the values of redox potentials were calibrated against the redox couple for ferrocene. This was done at the end of the CV measurements by adding $FeCp_2$ to the sample solution and measuring the $FeCp_2/FeCp_2^+$ redox couple under the conditions of the measurement in question. Cyclic voltammograms of complexes **2** and **4** with added $FeCp_2$ are shown in Figures S53 and S56 in the SI. We were surprised to note a dramatic color change, from pale yellow to black/dark green, upon addition of ferrocene to some of our cationic adducts. The rate of this color change varied from almost instantaneous to over minutes on ca. 10^{-4} M solutions. In addition, the CV traces of samples containing ferrocene also showed multiple redox features (see for instance Figures S53 and S56 in the SI). These observations prompted us to investigate the chemical reaction at its origin.

We began our investigation by examining those samples that did not appear to display this color change. Tests showed in fact that the same color change took place instantaneously when $FeCp_2$ was added to more concentrated solutions of these complexes. For instance, addition of 1.0 equiv of $FeCp_2$ to yellow (20−30) × 10^{-4} M $CDCl_3$ solutions of all cationic adducts (i.e., >20 times more concentrated than the samples used for CV measurements) led to immediate formation of a dark solution. Analysis of the resulting solution by ^{1}H NMR showed that the characteristic singlet resonance for the Cp protons of $FeCp_2$ (at 4.17 ppm) was absent from the spectrum. In addition, the spectrum displayed a number of ligand signals as well as a new signal that was very broad ($LW_{1/2}$ ∼500 Hz) and showed a variable intensity corresponding to between 4 and 7 protons depending on sample. The chemical shift of this new signal was also quite variable from one sample to another (10−6 ppm region), hinting that it might represent a paramagnetic species. Significantly, no reaction was apparent between the neutral bromide complexes **1**′−**6**′ and one or more equivalents of $FeCp_2$, confirming that the observed reaction takes place with the more electrophilic cationic adducts. Another piece of evidence supporting this proposal was furnished by the isolation of the oxidized species from a

DOI: 10.1021/acs.organomet.5b00272
Organometallics 2015, 34, 3520−3531

NMR sample, as follows: slow evaporation of a $CDCl_3$ solution containing the cationic adduct **3** and 2 equiv of ferrocene gave an amorphous green powder containing orange and dark-red crystals that were identified by X-ray crystallography as Cp_2Fe and $[Cp_2Fe][OTf]$, respectively.

The observed oxidation of ferrocene by our cationic Ni(II) complexes requires the concomitant reduction of the latter into charge-neutral, monovalent species; unfortunately, however, we have not succeeded in identifying the monovalent Ni product of the proposed redox reaction. Indeed, the following observation has indicated that the Ni-containing species might in fact be diamagnetic: the amorphous dark green solid obtained from the mixture of **8** and ferrocene showed a new ^{31}P NMR signal ($LW_{1/2}$ = 217 Hz) ca. 1−2 ppm upfield of the signal for the starting material.[26] This would rule out the formation of paramagnetic monomers of the type (R-POCOP$^{R'}$)Ni(NCMe). In conclusion, the fate of the Ni-containing species remains obscure at this point, but investigations are in progress to shed more light on this unexpected outcome.

Ligand-Exchange Studies. Previous reports in the context of Michael-type hydroamination of acrylonitrile promoted by pincer-Ni species have shown that the K_{eq} for the equilibrium $[(PCP^{iPr})Ni(NCMe)][BPh_4] \leftrightarrows [(PCP^{iPr})Ni(NCCHCH_2)][BPh_4]$ is near unity.[5a] This is an important consideration when discussing the mechanism of this catalytic reaction, because both the substrates and products feature nitrile moieties and their competitive binding can have an impact on catalytic turnover rates. On the other hand, in the context of Ni-catalyzed nitrile amidinations, the in situ generated amidine products are much more strongly donating ligands relative to nitrile substrates, a phenomenon that can lead to product inhibition, especially during the later phases of the catalytic process. Thus, in cationic adducts $[(pincer)NiL][OSO_2CF_3]$ the kinetic lability of the Ni−L moiety can influence catalytic turnover rates.

In contrast to the above cases involving the substitution of neutral donors L in $[(pincer)NiL][OSO_2CF_3]$ by other neutral donors L′, little is known about the substitutional lability of the corresponding Ni−X bond in the charge-neutral species (pincer)NiX (X = halides, OR, NR_2, etc.). We know, of course, that halide exchange by other halides or pseudohalides is possible in the presence of excess salts MX′ and that this type of exchange is usually more facile in polar solvents. We also know that halides can be displaced by charge-neutral nucleophiles L, but in most cases this is a less facile exchange that normally requires an abstracting agent such as Ag^+.

The question arose, what about halide/L exchange involving two complexes, a charge-neutral Ni−halide species and its cationic Ni−L analogue, $L_1NiX + [L_2NiL]^+ \leftrightarrows [L_1NiL]^+ + L_2NiX$? Although such ligand X/L exchanges are rarely considered, they can play a potentially important role in ionization of M−X moieties during catalytic reactions, thus affecting catalytic efficacy by creating resting states or dormant species. To shed some light on this issue, we have examined the ionization of the charge-neutral bromo species (R-POCOP$^{i\text{-}Pr}$)-NiBr in the presence of their cationic acetonitrile adducts [(R-POCOP$^{i\text{-}Pr}$)Ni(NCMe)][OSO_2CF_3], as depicted in eq 1. An interesting question to probe is whether the lability of the Ni−Br bond can be modulated by the nature of the POCOP ring substituent R.

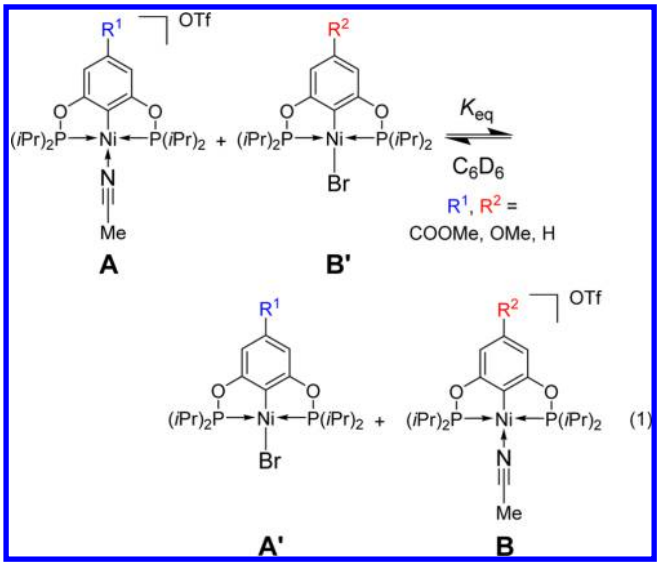

The predicted observation of near-unity K_{eq} values obtained for the exchange of precursors **A** and **B**′ bearing the same substituents R (Table 4: entries 1, 2, and 3) served to confirm

Table 4. Equilibrium Ligand Exchange as Per Eq 1[a]

entry	**A** (R^1)	**B**′ (R^2)	K_{eq}
1	**1** (H)	**1**′ (H)	1.07
2	**4** (*p*-CO_2Me)	**4**′ (*p*-CO_2Me)	1.06
3	**3** (*p*-OMe)	**3**′ (*p*-OMe)	1.09
4	**3** (*p*-OMe)	**4**′ (*p*-CO_2Me)	0.32
5	**4** (*p*-CO_2Me)	**3**′ (*p*-OMe)	2.82
6	**4** (*p*-CO_2Me)	**1**′ (H)	1.87
7	**1** (H)	**4**′ (*p*-CO_2Me)	0.60
8	**1** (H)	**3**′ (*p*-OMe)	1.50
9	**3** (p-OMe)	**1**′ (H)	0.80

[a]Experimental conditions: ^1H NMR spectra were recorded for two equimolar C_6D_6 solutions of A(R^1) and B′(R^2) each containing 2 equiv of dodecane as an internal standard (total volume of each sample: 750 μL). The samples were then combined in one NMR tube and subjected to repeated ^1H NMR measurements over a 25 min interval. The K_{eq} values were determined based on the integration of the aromatic region signals with respect to the dodecane signals.

the reliability of the methodology. Inspection of the remaining data shows that the smallest K_{eq} value is obtained for the exchange of **4**′ and **3** (entry 4), i.e., when the bromo species bears an electron-withdrawing substituent R^1 and the cationic adduct bears an electron-donating substituent R^2. Conversely, the largest K_{eq} value is obtained from the exchange of **4** and **3**′ (entry 5), i.e., when the cationic adduct bears an electron-withdrawing substituent R^1 and the bromo species bears an electron-donating substituent R^2. These observations can be rationalized by considering that the more labile acetonitrile moiety should be found in the cationic complex bearing an electron-withdrawing substituent, and vice versa. This explanation is also consistent with the observations that the second largest K_{eq} value involves the exchange of **4** (entry 6), whereas the second smallest K_{eq} value involves the exchange of **4**′ (entry 7). Finally, that the exchange of **3**′ and **1** (entry 8) results in a greater K_{eq} than that of **1**′ and **3** (entry 9) further supports the above rationale.

We put the above rationale to test by studying the exchange of one of our electron-poor POCOP-based cationic adducts

DOI: 10.1021/acs.organomet.5b00272
Organometallics 2015, 34, 3520−3531

Scheme 2. Ligand Exchange Reaction between 8 and ($PC_{sp3}P$)Ni−Br

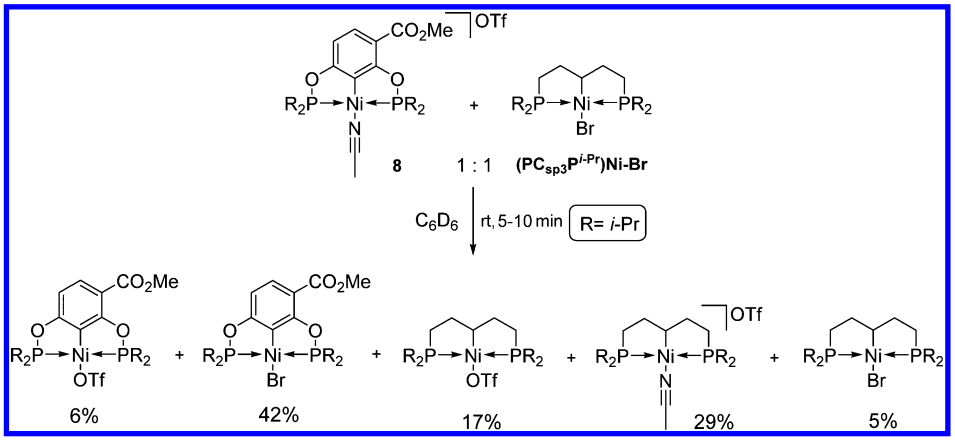

against a much more electron-rich charge-neutral bromo species, namely, van Koten's (NCN)Ni−Br (Scheme 2).[27] Exchange of the latter with complex **8** (R^2 = *m*-CO_2Me) led to an instantaneous reaction and gave a white precipitate. Analysis of the reaction mixture by ^{31}P NMR and ^{1}H NMR showed that the main product (~82%) was the charge-neutral bromide **8′** (two doublets at 190.43 and 192.12 ppm; J_{PP} = 323 Hz), confirming the facile ligand exchange between the starting materials (see Figures S66 and S67 in the SI). The reaction also generated side-products that displayed two apparent doublets; we believe that the latter represent the two central lines of poorly resolved AB signals, as follows. The first of these side-products displays two poorly resolved signals at 190.3 and 190.2 ppm, similar to the two peaks at 191.137 and 191.225 ppm in Figure S66 in the SI; this species (~18% relative intensity) was later identified as the charge-neutral triflate species (*m*-CO_2Me-POCOP)Ni-OTf (see below). The other side-product displays two poorly resolved signals at 187.9 and 187.8 ppm (~2% relative intensity) and remains unidentified. The observed white precipitate was identified as the cationic complex [(NCN)Ni(NCMe)][OSO_2CF_3] based on its characteristic ^{1}H NMR signal at 0.66 ppm for the coordinated acetonitrile.[28]

Next we studied another ligand exchange equilibrium involving the bromo complex ($PC_{sp3}P^{i\text{-}Pr}$)Ni−Br, a species for which the oxidation potential is lower than the values recorded for the POCOP systems **1**−**10**, but higher than that of van Koten's (NCN)Ni−Br. ^{31}P NMR analysis of a 1:1 mixture of ($PC_{sp3}P^{i\text{-}Pr}$)Ni−Br and the cationic adduct **8** showed the rapid establishment of an equilibrium mixture of five species, as shown in Scheme 2 (see Figure S68 in the SI for the spectrum). The assignment of the ^{31}P signals for (*m*-CO_2Me-POCOP)Ni−OTf was confirmed by adding to the reaction mixture an in situ generated sample from **8′** and AgOTf, as well as by adding a substoichiometric amount of AgOTf to the reaction mixture, which led to an increase in intensity of two signals for the triflate complexes (see Figure S69 in the SI for the spectrum with added AgOTf).[28]

The above observations establish that MeCN/Br^- ligand exchange between (R-$POCOP^{i\text{-}Pr}$)NiBr and [(R′-$POCOP^{i\text{-}Pr}$)Ni(NCMe)][OSO_2CF_3] takes place readily when the difference in the electronic proprieties of the aromatic ring substituents R and R′ is relatively small (entry 8 or 9). It is also noteworthy that the ligand exchange occurs in preference over other possible reactions. For instance, no redox reaction took place when we combined a very electron-poor complex such as [(*m*-CO_2Me-$POCOP^{i\text{-}Pr}$)Ni(NCMe)][OSO_2CF_3] (**8**) and a very electron-rich complex such as van Koten's (NCN)NiBr. A less electron-rich system also gives the ligand exchange, with two of the species being charge-neutral triflate derivatives.

CONCLUSIONS

This study has resulted in a number of interesting observations regarding the synthesis and stabilities of [(R-$POCOP^{R'}$)Ni(NCMe)][OSO_2CF_3] and has allowed us to study the impact of substituents R and R′ on the electrophilicity of the Ni center as reflected in ν(C≡N) values, redox potentials, and K_{eq} values for ligand exchange reactions with charge-neutral bromo complexes. The IR and CV measurements have confirmed the important influence of both *P*- and ring substituents on the electrophilicity of the Ni center in **1**−**10**. Both parameters show, for instance, that the most electrophilic adducts feature the *p*-CO_2Me substituent, but the redox potentials indicate that the Ni center ligated by *m*-CO_2Me-$POCOP^{i\text{-}Pr}$ is nearly as electrophilic. Indeed, the two sets of data lead to different conclusions regarding the electron density on Ni in the case of *t*-Bu_2P-based adducts: according to ν(C≡N) values, the Ni center is less electrophilic in [(*p*-CO_2Me-$POCOP^{t\text{-}Bu}$)Ni(NCMe)][OSO_2CF_3] (**10**) compared to its *i*-Pr_2P analogue; that is, the *t*-Bu_2P moiety is a stronger net donor, whereas the opposite conclusion is suggested by the redox potentials. Of course, the ν(C≡N) values were measured on solid samples, whereas the redox potentials are obtained from solutions; moreover, the fact that the redox events are irreversible in most cases (and certainly for the adducts bearing CO_2Me substituents) require us to treat the implications of the electrochemical data with caution.

The ligand exchange equilibrium studies demonstrated that coordinated acetonitrile ligands can be displaced by bromide and (to a lesser degree) triflate anions, and this substitution is more facile for the more electrophilic Ni center. This result indicates that the catalytic activities of cationic RCN adducts (e.g., acrylonitrile in hydroamination reactions or nitriles in amidination reactions) might be compromised in the presence of halides (used as "additives" in some settings) or other in situ generated anionic species (e.g., deprotonated amines or alcohols).

Finally, the present study revealed an unexpected side reaction between the cationic acetonitrile adducts and $FeCp_2$, presumably a redox reaction giving what we believe is a trivalent iron product. This intriguing possibility will be the

DOI: 10.1021/acs.organomet.5b00272
Organometallics 2015, 34, 3520−3531

subject of future investigations. We will also probe the catalytic reactivities of the cationic adducts **1**−**10** for hydroamination of acrylonitrile and its substituted derivatives, as well as for related transformations involving outer-sphere nucleophilic attack on the CN moiety (e.g., amidination and amidation).

EXPERIMENTAL SECTION

General Procedures. Unless otherwise indicated, all manipulations were carried out under a nitrogen atmosphere using standard Schlenk and glovebox techniques. The solvents were dried by passage over activated alumina contained in MBRAUN-SPS systems and analyzed by a Coulorimetric Karl Fischer titrator to acceptable water content. Triethylamine was dried by distillation over CaH_2. The following reagents and NMR solvents were purchased from Sigma-Aldrich and used without further purification: nickel powder, bromine, ClP(*i*-Pr)$_2$, ClP(*t*-Bu)$_2$, resorcinol, orcinol, 5-methyl-1,3-benzenediol, methyl 3,5-dihydroxybenzoate, methyl 2,4-dihydroxybenzoate, 4,6-di-*tert*-butylresorcinol, ferrocene, silver trifluoromethanesulfonate, C_6D_6, and $CDCl_3$. 5-Methoxyresorcinol was purchased from Chemsavers and used as received. 4-Methoxyresorcinol has been synthesized following a published procedure.[29] The precursor bromo complexes **1′**−**4′** and **6′**−**10′** were prepared following a previously reported procedure.[15a]

NMR spectra were recorded using the following Bruker spectrometers: AV300, AVII400, and AV500. Chemical shift values are reported in ppm (δ) and referenced internally to the residual solvent signals (^{1}H and ^{13}C: 7.26 and 77.16 ppm for $CDCl_3$; 7.16 and 128.06 ppm for C_6D_6) or externally (^{31}P, H_3PO_4 in D_2O, δ = 0). Coupling constants are reported in hertz. UV/vis spectra were recorded on a Varian Cary 500i. The IR spectra were recorded on a Bruker Alpha-P FTIR (4000−400 cm^{-1}). The elemental analyses were performed by the Laboratoire d'Analyse Élémentaire, Département de Chimie, Université de Montréal.

[{2,6-(*i*-Pr$_2$PO)$_2$-4-(Me)C$_6$H$_2$}Ni(NCMe)][OSO$_2$CF$_3$], 2. To an aluminum-foil-covered Schlenk flask containing **2′** (400 mg, 0.810 mmol, 1.00 equiv) in dry acetonitrile (20.0 mL) was added silver triflate (250 mg, 0.972 mmol, 1.20 equiv) at rt. The solution was then agitated for 3 h, filtered to remove the insoluble silver salts, and evaporated, and the resulting solids were extracted with dichloromethane (10.0 mL) and passed through a short Celite pad to remove the remaining traces of silver salts. Evaporation of the filtrate gave the desired product as a yellow solid (440 mg, 93%). Single crystals suitable for X-ray diffraction were obtained by slow evaporation in air by layering a $CDCl_3$ solution with hexanes. ^{1}H NMR (400 MHz, $CDCl_3$): δ 1.34 (appq*, ^3J = 7, 12H, P(CHC(C$\underline{H}_3$)$_2$)$_2$), 1.41 (appq, ^vJ = 8, 12H, P(CHC(C$\underline{H}_3$)$_2$)$_2$), 2.23 (s, 3H, C$_{Ar}$C$\underline{H}_3$), 2.42 (s(br), 3H, NCC$\underline{H}_3$), 2.52 (sept, $^3J_{HH}$ = 7, 4H, P(C$\underline{H}$C(CH$_3$)$_2$)$_4$), 6.28 (s, 2H, (C$_{Ar}\underline{H}_{meta}$)$_2$). ^{31}P{^{1}H} NMR (202 MHz, $CDCl_3$) δ: 193.4 (s). ^{19}F{^{1}H} NMR (282 MHz, $CDCl_3$): δ −78.06 (s). ^{13}C{^{1}H} NMR (75 MHz, $CDCl_3$): δ 3.91 (s(br), 1C, NC$\underline{C}$H$_3$), 16.87 (s, 4C, P(CH(C$\underline{H}_3$)$_2$)$_2$), 17.68 (vt, $^vJ_{PC}$ = 3, 4C, P(CH(C$\underline{H}_3$)$_2$)$_2$), 21.66 (s, 1C, C$_{Ar}$C$\underline{H}_3$), 28.52 (vt, $^vJ_{PC}$ = 12, 4C, P(C$\underline{H}$(CH$_3$)$_2$)$_4$), 107.18 (vt, $^vJ_{PC}$ = 6, 2C, C$_{Ar}\underline{H}$), 142.55 (s, 1C, C$_{Ar}\underline{C}$H$_3$), 168.92 (vt, $^vJ_{PC}$ = 9, 2C, (C$_{Ar}\underline{C}$OP)$_2$). IR (solid state, cm^{-1}): 636 (SO), 1030 (SO$_3$), 1141 (CF$_3$), 1262 (SO$_3$), 1464 (C═C^{Ar}), 1555 (C═C^{Ar}), 2294 (C≡N). UV−vis ((CH$_2$Cl$_2$, [1 × 10^{-4} M]), λ_{max}, nm (ε, L mol^{-1} cm^{-1}): 242 (11 878), 300 (2302), 327 (2691), 386 (711). E-chem (NBu$_4$PF$_6$, 10^{-4} M in dry CH$_2$Cl$_2$, E_{ox} vs FeCp$_2$): 1151 mV. Elemental analysis was not satisfactory for this complex, because it proved difficult to remove all traces of solvents. *appq refers to an apparent quartet signal resulting from two overlapping virtual triplets.

[{2,6-(*i*-Pr$_2$PO)$_2$-4-(OMe)C$_6$H$_2$}Ni(NCMe)][OSO$_2$CF$_3$], 3. The procedure described above for the preparation of **2** was used for this synthesis using **3′** (415 mg, 0.812 mmol, 1.00 equiv). The desired product was obtained as a yellow solid (415 mg, 84%). Single crystals suitable for X-ray diffraction were obtained by slow evaporation in air of an acetone solution layered with hexanes. ^{1}H NMR (400 MHz, $CDCl_3$): δ 1.35 (appq, ^vJ = 8, 12H, P(CHC(C$\underline{H}_3$)$_2$)$_2$), 1.41 (appq, ^vJ = 8, 12H, P(CHC(C$\underline{H}_3$)$_2$)$_2$), 2.39 (s(br), 3H, NCC$\underline{H}_3$), 2.52 (sept, $^3J_{HH}$ = 8, 4H, P(C$\underline{H}$C(CH$_3$)$_2$)$_4$), 3.73 (s, 3H, OC$\underline{H}_3$), 6.08 (s, 2H, (C$_{Ar}\underline{H}_{meta}$)$_2$). ^{31}P{^{1}H} NMR (121 MHz, $CDCl_3$): δ 191.6 (s). ^{19}F{^{1}H} NMR ($CDCl_3$, 282 MHz): δ −77.94 (s). ^{13}C{^{1}H} NMR (125 MHz, $CDCl_3$): δ 3.98 (s(br), 1C, NC$\underline{C}$H$_3$), 16.82 (s, 4C, P(CH(C$\underline{H}_3$)$_2$)$_4$), 17.61 (s(br), 4C, P(CH(C$\underline{H}_3$)$_2$)$_2$), 28.52 (vt, $^vJ_{PC}$ = 12, 4C, P(C$\underline{H}$(CH$_3$)$_2$)$_4$), 55.67 (s, 1C, OC$\underline{H}_3$), 93.22 (vt, $^vJ_{PC}$ = 7, 2C, C$_{Ar}\underline{H}$), 163.47 (s, 1C, C$_{Ar}\underline{C}$OCH$_3$), 169.31 (vt, $^vJ_{PC}$ = 9, 2C, (C$_{Ar}\underline{C}$OP)$_2$). IR (solid state, cm^{-1}): 636 (SO), 1030 (SO$_3$), 1140 (CF$_3$), 1266 (SO$_3$), 1462 (C═C^{Ar}), 1561 (C═C^{Ar}), 2293 (C≡N). UV−vis ((CH$_2$Cl$_2$, [1 × 10^{-4} M]), λ_{max}, nm (ε, L mol^{-1} cm^{-1}): 243 (12 834), 299 (1858), 329 (4214), 382 (912). E-chem (NBu$_4$PF$_6$, 10^{-4} M in dry CH$_2$Cl$_2$, E_{ox} vs FeCp$_2$ [$E_{1/2}$ vs FeCp$_2$]): 933 mV [922 mV]. Anal. Calcd for $C_{22}H_{36}F_3NNiO_6P_2S$ (620.22): C, 42.60; H, 5.85; N, 2.26; S, 5.17. Found: C, 42.83; H, 5.85; N, 1.97; S, 5.20.

[{2,6-(*i*-Pr$_2$PO)$_2$-4-(CO$_2$Me)C$_6$H$_2$}Ni(II)(NCMe)][OSO$_2$CF$_3$], 4. The procedure described above for the preparation of **2** was used for this synthesis using **4′** (204 mg, 0.379 mmol, 1.00 equiv). The desired product was obtained as a yellow solid (189 mg, 81%). Single crystals suitable for X-ray diffraction were obtained by slow evaporation in air of a dichloromethane solution layered with hexanes. ^{1}H NMR (300 MHz, $CDCl_3$): δ 1.38 (m, 24H, P(CHC(C$\underline{H}_3$)$_2$)$_4$), 2.52 (s, 3H, NCC$\underline{H}_3$), 2.57 (m, 4H, P(C$\underline{H}$C(CH$_3$)$_2$)$_4$), 3.85 (s, 3H, C(O)OC$\underline{H}_3$), 7.10 (s, 2H, C$_{Ar}\underline{H}$). ^{31}P{^{1}H} NMR (161 MHz, $CDCl_3$): δ 196.4 (s). ^{19}F{^{1}H} NMR ($CDCl_3$, 282 MHz): δ −78.17 (s). ^{13}C{^{1}H} NMR (75 MHz, $CDCl_3$): δ 4.18 (s(br), 1C, NC$\underline{C}$H$_3$), 16.80 (s, 4C, P(CH(C$\underline{H}_3$)$_2$)$_2$), 17.59 (vt, $^vJ_{PC}$ = 3, 4C, P(CH(C$\underline{H}_3$)$_2$)$_2$), 28.62 (vt, $^vJ_{PC}$ = 11, 4C, P(C$\underline{H}$(CH$_3$)$_2$)$_4$), 52.41 (s, 1C, OC$\underline{H}_3$), 106.24 (t, J_{PC} = 7, 1C, C$_{ipso}\underline{C}$Ni), 107.12 (vt, $^vJ_{PC}$ = 6, 2C, C$_{Ar}\underline{H}$), 133.30 (s, 1C, C$_{Ar}\underline{C}$(O)OCH$_3$), 166.22 (s, 1C, C$_{Ar}\underline{C}$(O)OCH$_3$), 168.85 (vt, $^vJ_{PC}$ = 9, 2C, (C$_{Ar}\underline{C}$OP)$_2$). IR (solid state, cm^{-1}): 635 (SO), 1029 (SO$_3$), 1140 (CF$_3$), 1277 (SO$_3$), 1397 (C═C^{Ar}), 1550 (C═C^{Ar}), 1716 (C═O), 2329 (C≡N). UV−vis ((CH$_2$Cl$_2$, [1 × 10^{-4} M]), λ_{max}, nm (ε, L mol^{-1} cm^{-1}): 248 (11 577), 329 (4791), 341 (5111, 390 (1697). E-chem (NBu$_4$PF$_6$, 10^{-4} M in dry CH$_2$Cl$_2$, E_{ox} vs FeCp$_2$): 1269 mV. Anal. Calcd for $C_{23}H_{36}F_3NNiO_7P_2S$ (648.24): C, 42.62; H, 5.60; N, 2.16; S, 4.95. Found: C, 43.10; H, 5.71; N, 1.98; S, 4.65.

[{2,6-(*i*-Pr$_2$PO)$_2$-4-(Br)C$_6$H$_2$}Ni(NCMe)][OSO$_2$CF$_3$], 5. The procedure described above for the preparation of **2** was used for this synthesis using **5′** (400 mg, 0.716 mmol, 1.00 equiv). The desired product was obtained as a yellow solid (412 mg, 86%). Crystals suitable for diffraction studies were obtained by slow evaporation in air of a dichloromethane solution layered with hexanes. ^{1}H NMR (500 MHz, $CDCl_3$): δ 1.32 (appq, ^vJ = 9, 12H, P(CH(C$\underline{H}_3$)$_2$)$_2$), 1.37 (appq, ^vJ = 8, 12H, P(CH(C$\underline{H}_3$)$_2$)$_2$), 2.37 (s(br), 3H, NCC$\underline{H}_3$), 2.55 (sept, $^3J_{HH}$ = 7, 4H, P(C$\underline{H}$(CH$_3$)$_2$)$_4$), 6.64 (s, 2H, C$_{Ar}\underline{H}$). ^{31}P{^{1}H} NMR (161 MHz, $CDCl_3$): δ 195.7 (s). ^{19}F{^{1}H} NMR (282 MHz, $CDCl_3$): δ −77.79 (s). ^{13}C{^{1}H} NMR (75 MHz, $CDCl_3$): δ 3.84 (s(br), 1C, NC$\underline{C}$H$_3$), 16.76 (s, 4C, P(CH(C$\underline{H}_3$)$_2$)$_2$), 17.57 (vt, $^vJ_{PC}$ = 3, 4C, P(CH(C$\underline{H}_3$)$_2$)$_2$), 28.58 (vt, $^vJ_{PC}$ = 12, 4C, P(C$\underline{H}$(CH$_3$)$_2$)$_4$), 110.01 (vt, $^vJ_{PC}$ = 6, 2C, C$_{Ar}\underline{C}$H$_{meta}$), 123.54 (s, 1C, C$_{Ar}\underline{C}$Br), 168.93 (vt, $^vJ_{PC}$ = 9, 2C, (C$_{Ar}\underline{C}$OP)$_2$). IR (solid state, cm^{-1}): 637 (SO), 1032 (SO$_3$), 1142 (CF$_3$), 1264 (SO$_3$), 1466 (C═C^{Ar}), 1554 (C═C^{Ar}), 2302 (C≡N). UV−vis ((CH$_2$Cl$_2$, [1 × 10^{-4} M]), λ_{max}, nm (ε, L mol^{-1} cm^{-1}): 243 (15 984), 303 (3547), 328 (6245), 386 (1221). E-chem (NBu$_4$PF$_6$, 10^{-4} M in dry CH$_2$Cl$_2$, E_{ox} vs FeCp$_2$): 1159 mV. Anal. Calcd for $C_{24}H_{42}BrNNiO_5P_2S$ (655.08): C, 37.70; H, 4.97; N, 2.08; S, 4.79. Found: C, 37.79; H, 4.93; N, 2.04; S, 4.71.

{2,6-(*i*-Pr$_2$PO)$_2$-4-(Br)C$_6$H$_2$}NiBr, 5′. This compound was prepared by adapting a literature procedure.[18] In a 500 mL round-bottom flask containing 1-bromo-3,5-dimethoxybenzene (6.40 g, 29.5 mmol) was added HBr (100 mL), to which was attached a condenser under nitrogen. The heterogeneous solution was stirred and heated for 24 h at 120 °C. The solution was then cooled and treated with anhydrous $KHCO_3$ until the evolution of CO_2 ceased and a precipitate formed. The precipitate was filtered, washed with water, and dried under vacuum at 80 °C, yielding the known 5-bromoresorcinol as a pale pink solid (4.77 g, 85%). A dry Schlenk flask charged in the glovebox with 5-bromoresorcinol (1.00 g, 5.20 mmol in 50 mL) and chlorodiisopropylphosphine (1.77 mL, 11.1 mmol) was taken out of the box, and to the contents were added dry THF (50.0 mL) and triethylamine

DOI: 10.1021/acs.organomet.5b00272
Organometallics 2015, 34, 3520−3531

(1.57 mL, 11.6 mmol). The mixture was stirred for 1 h at rt, while the ammonium salt precipitated as a white solid. Evaporation, followed by extraction with dry hexane (50.0 mL) and evaporation, gave the crude product as a pale yellow oil (1.52 g, ca. 68%). The ^{31}P NMR spectrum of this material showed it to contain the desired product as the major product, in addition to minor quantities of oxidized phosphines. Reaction of the crude sample of the ligand (1.52 g, ca. 3.61 mmol) with the nickel precursor $NiBr_2(NCCH_3)_2$ (1.30 g, 4.32 mmol) in dry THF (50 mL) and in the presence of dry triethylamine (0.630 mL, 4.69 mmol) gave a dark green suspension. Stirring for 1 h at rt, followed by evaporation and extraction with dry hexane (50.0 mL), gave brown crystals of the desired product (1.21 g, 60%) after crystallization in air. ^{1}H NMR (400 MHz, C_6D_6): δ 1.08 (appq, ^vJ = 7, 12H, $P(CH(CH_3)_2)_2$), 1.32 (appq, ^vJ = 8, 12H, $P(CH(CH_3)_2)_2$), 2.16 (sept, $^3J_{HH}$ = 7, 4H, $P(CH(CH_3)_2)_4$), 6.80 (s, 2H, $C_{Ar}H$). ^{31}P{^{1}H} NMR (161 MHz, C_6D_6): δ 190.8 (s). ^{13}C{^{1}H} NMR (75 MHz, C_6D_6): δ 16.61 (s, 4C, $P(CH(CH_3)_2)_2$), 17.69 (s, 4C, $P(CH(CH_3)_2)_2$), 28.24 (vt, $^vJ_{PC}$ = 11, 4C, $P(CH(CH_3)_2)_4$), 109.40 (vt, $^vJ_{PC}$ = 6, 1C, $C_{Ar}H_{meta}$), 121.42 (s, 1C, $C_{Ar}Br$), 169.20 (vt, $^vJ_{PC}$ = 10, 2C, $(C_{Ar}OP)_2$). UV−vis ($(CH_2Cl_2$, [1 × 10^{-4} M]), λ_{max}, nm (ε, mol^{-1} cm^{-2}): 266 (6360), 306 (2900), 341 (13 600), 391 (2070). E-chem (NBu_4PF_6, 10^{-4} M in dry CH_2Cl_2, E_{ox} vs $FeCp_2$): 738 mV. Anal. Calcd for $C_{18}H_{30}Br_2NiO_2P_2$ (558.88 g/mol): C, 38.68; H, 5.41. Found: C, 39.30; H, 5.59.

[{2,6-(*i*-$Pr_2PO)_2$-3,5-(*t*-Bu)$_2C_6H$}Ni(II)(NCMe)][OSO_2CF_3], 6. The procedure described above for the preparation of **2** was used for this synthesis using **6′** (407 mg, 0.686 mmol, 1.00 equiv). The desired product was obtained as a yellow solid (410 mg, 87%). The crystals were obtained by slow evaporation in air of the solid dissolved in acetonitrile. ^{1}H NMR (300 MHz, $CDCl_3$): δ 1.29 (s, 18H, $(C_{Ar}(CH_3)_3)_2$), 1.31−1.42 (m, 24H, $P(CHC(CH_3)_2)_4$), 2.38 (s(br), 3H, $NCCH_3$), 2.55 (m(br), 4H, $P(CHC(CH_3)_2)_4$), 7.00 (s, 1H, $C_{Ar}H$). ^{31}P{^{1}H} NMR (161 MHz, $CDCl_3$): δ 192.9 (s). ^{19}F{^{1}H} NMR ($CDCl_3$, 282 MHz): δ −78.04 (s). ^{13}C{^{1}H} NMR (75 MHz, $CDCl_3$): δ 4.22 (s, 1C, $NCCH_3$), 8.94 (s, 1C, $NCCH_3$), 16.97 (s, 4C, $P(CH(CH_3)_2)_2$), 17.62 (vt, $^vJ_{PC}$ = 3, 4C, $P(CH(CH_3)_2)_2$), 28.43 (vt, $^vJ_{PC}$ = 12, 4C, $P(CH(CH_3)_2)_4$), 29.82 (s, 6C, $(C_{Ar}(C(CH_3)_3)_2)$, 34.42 (s, 4C, $(C_{Ar}(C(CH_3)_3)_4)$, 126.31 (s, 1C, $C_{Ar}H$), 127.66 (vt, $^vJ_{PC}$ = 5, 2C, $(C_{Ar}(C(CH_3)_3))_2$) 164.36 (vt, $^vJ_{PC}$ = 11, 2C, $(C_{Ar}OP)_2$). IR (solid state, cm^{-1}): 636 (SO), 1028 (SO_3), 1143 (CF_3), 1251 (SO_3), 1459 (C═C_{Ar}), 1552 (C═C_{Ar}), 2294 (C≡N). UV−vis (CH_2Cl_2, [1 × 10^{-4} M], λ_{max}, nm (ε, L mol^{-1} cm^{-1})): 299 (2432), 327 (2691), 386 (711). E-chem (NBu_4PF_6, 10^{-4} M in dry CH_2Cl_2, E_{ox} vs $FeCp_2$ [$E_{1/2}$ vs $FeCp_2$]): 1012 mV [997 mV]. Anal. Calcd for $C_{29}H_{50}F_3NNiO_5P_2S$ (702.41): C, 49.59; H, 7.17; N, 1.99; S, 4.56. Found: C, 49.30; H, 7.23; N, 1.95; S, 4.77.

[{2,6-(*i*-$Pr_2PO)_2$-3-(OMe)C_6H_2}Ni(NCMe)][OSO_2CF_3], 7. The procedure described above for the preparation of **2** was used for this synthesis using **7′** (201 mg, 0.395 mmol, 1.00 equiv). The desired product was obtained as a yellow solid that was evaporated from a yellow oil (188 mg, 81%). ^{1}H NMR (400 MHz, $CDCl_3$): δ 1.25−1.37 (m, 24H, $P(CHC(CH_3)_2)_4$), 2.38 (s(br), 3H, $NCCH_3$), 2.61−2.43 (m, 4H, $P(CH(CH_3)_2)_4$), 3.72 (s, 3H, OCH_3), 6.35 (d, $^3J_{HH}$ = 9, 1H, $C_{Ar}H_{meta}$), 6.64 (d, $^3J_{HH}$ = 9, 1H, $C_{Ar}H_{para}$). ^{19}F NMR (282 MHz, $CDCl_3$): δ −78.20 (s). ^{31}P{^{1}H} NMR (161 MHz, $CDCl_3$): δ 195.7 (d, J_{PP} = 258, 1P), 191.39 (d, J_{PP} = 258, 1P). ^{13}C NMR (101 MHz, $CDCl_3$): δ 3.53 (s, 1C, $NCCH_3$), 16.65 (s, 2C, $P(CH(CH_3)_2)$, 16.78 (s, 2C, $P(CH(CH_3)_2)$) 17.46 (s, 2C, $P(CH(CH_3)_2)$), 17.52 (s, 2C, $P(CH(CH_3)_2)$), 28.57 (ABX, $^1J_{PC}$ + $^3J_{PC}$ = 22, 2C, $P(CH(CH_3)_2)_2$), 28.37 (ABX, $^1J_{PC}$ + $^3J_{PC}$ = 22, 2C, $P(CH(CH_3)_2)_2$), 56.98 (s, 1C, OCH_3), 105.03 (d, $^3J_{PC}$ = 13, 1C, $C_{Ar}H_{meta}$), 115.11 (s, 1C, $C_{Ar}H_{para}$), 123.82 (t, $^2J_{PC}$ = 20, NiC_{ipso}), 140.98 (d, $^3J_{PC}$ = 15, 1C, $C_{Ar}OCH_3$), 157.21 (dd, $^2J_{PC}$ = 13; $^4J_{PC}$ = 6, 1C, $C_{Ar}OP$), 162.52 (dd, $^2J_{PC}$ = 11; $^4J_{PC}$ =7, 1C, $C_{Ar}OP$). IR (solid state, cm^{-1}): 634 (SO), 1027 (SO_3), 1144 (CF_3), 1259 (SO_3), 1461 (C═C^{Ar}), 1570 (C═C^{Ar}), 2284 (C≡N). UV−vis ($(CH_2Cl_2$, [1 × 10^{-4} M]), λ_{max}, nm (ε, L mol^{-1} cm^{-1}): 279 (17 577), 323 (11 373), 384 (1881) . E-chem (NBu_4PF_6, 10^{-4} M in dry CH_2Cl_2, E_{ox} vs $FeCp_2$ [$E_{1/2}$ vs $FeCp_2$]): 938 mV [967 mV]. Anal. Calcd for $C_{22}H_{36}F_3NNiO_6P_2S$ (620.23): C, 42.60; H, 5.85; N, 2.26; S, 5.17. Found: C, 42.36; H 6.00; N, 2.11; S, 5.29.

[{2,6-(*i*-$Pr_2PO)_2$-3-(CO_2Me)C_6H_2}Ni(NCMe)][OSO_2CF_3], 8. The procedure described above for the preparation of **2** was used for this synthesis using **8′** (405 mg, 0.752 mmol, 1.00 equiv). The desired product was obtained as an orange solid that was in turn obtained by evaporation in air from an orange oil (360 mg, 89%). ^{1}H NMR (500 MHz, $CDCl_3$): δ 1.31−1.41 (m, 24H, $P(CHC(CH_3)_2)_4$), 2.46 (s, 3H, $NCCH_3$), 2.59 (sept, $^3J_{HH}$ = 4, 4H, $P(CHC(CH_3)_2)_4$), 3.82 (s, 3H, $C(O)OCH_3$), 6.52 (d, $^3J_{HH}$ = 8, 1H, $C_{Ar}H_{meta}$), 7.72 (d, $^3J_{HH}$ = 8, $C_{Ar}H_{para}$). ^{31}P{^{1}H} NMR (202 MHz, $CDCl_3$): δ 195.3 (s). ^{19}F{^{1}H} NMR ($CDCl_3$, 282 MHz): δ −77.80 (s). ^{13}C{^{1}H} NMR (125 MHz, $CDCl_3$): δ 4.26 (s(br), 1C, $NCCH_3$), 8.90 (s, 1C, $NCCH_3$), 16.79 (s, 2C, $P(CH(CH_3)_2)$), 16.90 (s, 2C, $P(CH(CH_3)_2)$), 17.58 (vt $^vJ_{PC}$ = 2, 2C, $P(CH(CH_3)_2)$), 17.69 (vt, $^vJ_{PC}$ = 2, 2C, $P(CH(CH_3)_2)$), 28.59 (ABX, $^1J_{PC}$ + $^3J_{PC}$ = 33, 2C, $P(CH(CH_3)_2)_2$), 28.67 (ABX, $^1J_{PC}$ + $^3J_{PC}$ = 32, 2C, $P(CH(CH_3)_2)_2$), 51.96 (s, 1C, $C(O)OCH_3$), 106.79 (dd, $^3J_{PC}$= 7, $^5J_{PC}$ = 4; 1C, $C_{Ar}H_{meta}$), 110.64 (dd, $^3J_{PC}$= 7, $^5J_{PC}$ = 5; 1C, $C_{Ar}H_{para}$), 134.38 (s, 1C, $C_{Ar}C(O)OCH_3$)), 165.12 (s, 1C, $C_{Ar}C(O)OCH_3$), 168.30 (vt, $^vJ_{PC}$ = 9, 1C, C_{Ar} (OP)), 171.91 (vt, $^vJ_{PC}$ = 8, 1C, $C_{Ar}OP$). IR (solid state, cm^{-1}): 637 (SO), 1032 (SO_3), 1149 (CF_3), 1272 (SO_3), 1383 (C═C^{Ar}), 1578 (C═C^{Ar}), 1712 (C═O), 2303 (C≡N). E-chem (NBu_4PF_6, 10^{-4} M in dry CH_2Cl_2, E_{ox} vs $FeCp_2$): 1262 mV. UV−vis (CH_2Cl_2,[1 × 10^{-4} M], λ_{max}, nm (ε, L mol^{-1} cm^{-1})): 249 (30 114), 327 (12 630), 346 (2461). Elemental analysis was not satisfactory for this complex, because it proved difficult to remove all traces of solvents.

[{2,6-(*t*-$Bu_2PO)_2C_6H_3$}Ni(NCMe)][OSO_2CF_3], 9. The procedure described above for the preparation of **2** was used for this synthesis using **9′** (157 mg, 0.293 mmol, 1.00 equiv). The desired product was obtained as a yellow solid (178 mg, 94%). Single crystals suitable for X-ray diffraction were obtained by slow evaporation in air from a dichloromethane solution layered with hexanes. ^{1}H NMR (500 MHz, $CDCl_3$): δ 1.44 (vt, $^vJ_{PH}$ = 5, 36H, $P(C(CH_3)_3)_4$), 2.67 (s(br), 3H, $NCCH_3$), 6.47 (d, $^3J_{HH}$ = 10, 2H, $(C_{Ar}H_{meta})_2$), 7.03 (t, $^3J_{HH}$ = 8, 1H, $C_{Ar}H_{para}$). ^{31}P{^{1}H} NMR (121 MHz, $CDCl_3$): δ 197.8 (s). ^{19}F{^{1}H} NMR (282 MHz, $CDCl_3$): δ −77.64(s). ^{13}C{^{1}H} NMR (125 MHz, $CDCl_3$): δ 4.51 (s(br), 1C, $NCCH_3$), 27.87 (s(br), 12C, $P(C(CH_3)_3)_4$), 40.02 (vt, $^vJ_{PC}$ = 8, 4C, $P(C(CH_3)_3)_4$), 106.21 (vt, $^vJ_{PC}$ = 6, 2C, $(C_{Ar}H_{meta})_2$), 122.53 (t, $^2J_{PC}$ = 19, 1C, $C_{ipso}Ni$), 131.10 (s, 1C, $C_{Ar}H_{para}$), 135.89 (s, 1C, OSO_2CF_3), 169.70 (vt, $^vJ_{PC}$ = 8, 2C, $(C_{Ar}OP)_2$). IR (solid state, cm^{-1}): 635 (SO), 1027 (SO_3), 1144 (CF_3), 1263 (SO_3), 1477 (C═C^{Ar}), 1558 (C═C^{Ar}), 2293 (C≡N). E-chem (NBu_4PF_6, 10^{-4} M in dry CH_2Cl_2, E_{ox} vs $FeCp_2$): 1298 mV. UV−vis ($(CH_2Cl_2$, [1 × 10^{-4} M]), λ_{max}, nm (ε, L mol^{-1} cm^{-1})): 258 (15464), 321 (9449), 338 (sh, 2378), 401 (305). Elemental analysis was not satisfactory for this complex, because it proved difficult to remove all traces of solvents.

[{2,6-(*t*-$Bu_2PO)_2$-4-(CO_2Me)C_6H_2}Ni(NCMe)][OSO_2CF_3], 10. The procedure described above for the preparation of **2** was used for this synthesis using **10′** (270 mg, 0.455 mmol, 1.00 equiv). The desired product was obtained as a yellow solid (256 mg, 80%). Single crystals suitable for X-ray diffraction were obtained by slow evaporation in air from a solution of $CDCl_3$ layered with hexanes. ^{1}H NMR (500 MHz, $CDCl_3$): δ 1.45 (vt, $^vJ_{PH}$ = 8, 36H, $P(C(CH_3)_3)_4$), 2.70 (s, 3H, $NCCH_3$), 3.87 (s, 3H, $C_{Ar}COOCH_3$), 7.14 (s, 2H, $C_{Ar}H_{meta}$). ^{31}P{^{1}H} NMR (202 MHz, $CDCl_3$): δ 199.3 (s). ^{19}F{^{1}H} NMR (470 MHz, $CDCl_3$): δ −77.96 (s). ^{13}C{^{1}H} NMR (125 MHz, $CDCl_3$): δ 4.66 (s, 1C, $NCCH_3$), 27.84 (s, 12C, $P(C(CH_3)_3)_4$), 40.28 (vt, $^vJ_{PC}$ = 8, 4C, $P(C(CH_3)_3)_4$), 52.47 (s, 1C, OCH_3), 107.14 (vt, $^vJ_{PC}$ = 6, 2C, $(C_{Ar}H_{meta})_2$), 129.81 (t, $^2J_{PC}$ = 19, 1C, $C_{ipso}Ni$), 133.28 (s, 1C, $C_{Ar}CO_2CH_3$), 136.70 (s, 1C, OSO_2CF_3), 166.19 (s, 1C, $C_{Ar}CO_2CH_3$), 169.41 (vt, $^vJ_{PC}$ = 8, 2C, $(C_{Ar}OP)_2$). IR (solid state, cm^{-1}): 635 (SO), 1032 (SO_3), 1135 (CF_3), 1270 (SO_3), 1397 (C═C^{Ar}), 1552 (C═C^{Ar}), 1715 (C═O), 2315 (C≡N). E-chem (NBu_4PF_6, 10^{-4} M in dry CH_2Cl_2, E_{ox} vs $FeCp_2$): 1457 mV. UV−vis ($(CH_2Cl_2$, [1 × 10^{-4} M]), λ_{max}, nm (ε, L mol^{-1} cm^{-1}): 257 (19 757), 335 (18 544), 400 (718). Elemental analysis was not satisfactory for this complex, because it proved difficult to remove all traces of solvents.

DOI: 10.1021/acs.organomet.5b00272
Organometallics 2015, 34, 3520−3531

■ ASSOCIATED CONTENT

Supporting Information

Tables of crystal data and collection/refinement parameters; table of additional distances and angles for complexes **1**−**10** and **5**′; figures of molecular diagrams for complexes **2**, **3**, **5**, **5**′, and **9**; ^{1}H, ^{31}P, and ^{13}C NMR spectra of complexes **1**−**10**; table with detailed IR frequency assignments for complexes **1**−**10**; additional information for IR, electrochemical, and ligand-exchange studies. Complete details of the X-ray analyses reported herein have been deposited at the Cambridge Crystallographic Data Center (CCDC 1044410 (**2**), 942873 (**3**), 942874 (**4**), 942876 (**5**), 942875 (**5**′), 942877 (**6**), 1044411 (**9**), 1044412 (**10**)). These data can be obtained free of charge via www.ccdc.cam.ac.uk/data_request/cif, or by e-mailing data_request@ccdc.cam.ac.uk or by contacting the Cambridge Crystallographic Data Centre, 12 Union Road, Cambridge CD2 1EZ, UK; fax: +44 1223 336033. The Supporting Information is available free of charge on the ACS Publications website at DOI: 10.1021/acs.organomet.5b00272.

■ AUTHOR INFORMATION

Corresponding Author

*E-mail: zargarian.davit@umontreal.ca.

Present Address

[†]Department of Chemistry, Texas A&M University, College Station, Texas 77843-3255, United States.

Notes

The authors declare no competing financial interest.

■ ACKNOWLEDGMENTS

The authors are grateful to NSERC of Canada for financial support of this work (Discovery and RTI grants to D.Z.); Université de Montréal (graduate fellowships to S.L.); Dr. Michel Simard and Ms. Francine Bélanger-Gariépy for their valuable assistance with crystallography and many interesting discussions; Ms. Elena Nadezhina for the elemental analyses; Dr. D. Rochefort for valuable advice regarding the electrochemical measurements; and the reviewers of our manuscript, who recommended that we measure the open-circuit (rest) potentials of our complexes and offered many valuable suggestions regarding the reporting of the NMR data. S.L. is also grateful to Centre in Green Chemistry and Catalysis for a travel award, to J.-P. Cloutier for the loan of complexes used in the ligand exchange studies, and to all group members for many valuable discussions and practical advice.

■ REFERENCES

(1) Moulton, C. J.; Shaw, B. L. *J. Chem. Soc., Dalton Trans.* **1976**, *11*, 1020−1024.

(2) (a) van Koten, G.; Jastrzebski, J. T. B. H.; Noltes, J. G.; Spek, A. L.; Schoone, J. C. *J. Organomet. Chem.* **1978**, *148* (3), 233−245. (b) van Koten, G.; Timmer, K.; Noltes, J. G.; Spek, A. L. *J. Chem. Soc., Chem. Commun.* **1978**, *6*, 250−252.

(3) Van Koten, G. *Pure Appl. Chem.* **1989**, *61* (10), 1681−94.

(4) (a) van Koten, G. *J. Organomet. Chem.* **2013**, *730*, 156−164. (b) van Koten, G. The Monoanionic ECE-Pincer Ligand: A Versatile Privileged Ligand Platform—General Considerations. In *Topics in Organometallic Chemistry*; van Koten, G.; Milstein, D., Eds.; Springer: Berlin, 2013; Vol. *40*, pp 1−20. (c) Morales-Morales, D.; Jensen, C. G. M. *The Chemistry of Pincer Compounds*; Elsevier Science, 2011. (d) Poverenov, E.; Milstein, D. Noninnocent Behavior of PCP and PCN Pincer Ligands of Late Metal Complexes. In *Topics in Organometallic Chemistry*, van Koten, G.; Milstein, D., Eds.; Springer: Berlin, 2013; Vol. *40*, pp 21−47. (e) Roddick, D. Tuning of PCP Pincer Ligand Electronic and Steric Properties. In *Topics in Organometallic Chemistry*; van Koten, G.; Milstein, D., Eds.; Springer: Berlin, 2013; Vol. *40*, pp 49−88.

(5) (a) Castonguay, A.; Sui-Seng, C.; Zargarian, D.; Beauchamp, A. L. *Organometallics* **2006**, *25* (3), 602−608. (b) Kennedy, A. R.; Cross, R. J.; Muir, K. W. *Inorg. Chim. Acta* **1995**, *231* (1−2), 195−200. (c) Huck, W. T. S.; Snellink-Ruël, B.; van Veggel, F. C. J. M.; Reinhoudt, D. N. *Organometallics* **1997**, *16* (20), 4287−4291. (d) Kozhanov, K. A.; Bubnov, M. P.; Cherkasov, V. K.; Fukin, G. K.; Abakumov, G. A. *Chem. Commun.* **2003**, *20*, 2610−2611. (e) Kozhanov, K. A.; Bubnov, M. P.; Cherkasov, V. K.; Vavilina, N. N.; Efremova, L. Y.; Artyushin, O. I.; Odinets, I. L.; Abakumov, G. A. *Dalton Trans.* **2008**, *21*, 2849−2853. (f) Cámpora, J.; Palma, P.; del Río, D.; Álvarez, E. *Organometallics* **2004**, *23* (8), 1652−1655. (g) Cámpora, J.; Palma, P.; del Río, D.; Conejo, M. M.; Álvarez, E. *Organometallics* **2004**, *23* (24), 5653−5655. (h) Castonguay, A.; Beauchamp, A. L.; Zargarian, D. *Organometallics* **2008**, *27* (21), 5723−5732. (i) Boro, B. J.; Duesler, E. N.; Goldberg, K. I.; Kemp, R. A. *Inorg. Chem.* **2009**, *48* (12), 5081−5087. (j) Groux, L. F.; Belanger-Gariepy, F.; Zargarian, D. *Can. J. Chem.* **2005**, *83* (6−7), 634−639. (k) Schmeier, T. J.; Hazari, N.; Incarvito, C. D.; Raskatov, J. A. *Chem. Commun.* **2011**, *47* (6), 1824−1826. (l) Levina, V. A.; Rossin, A.; Belkova, N. V.; Chierotti, M. R.; Epstein, L. M.; Filippov, O. A.; Gobetto, R.; Gonsalvi, L.; Lledós, A.; Shubina, E. S.; Zanobini, F.; Peruzzini, M. *Angew. Chem., Int. Ed.* **2011**, *50* (6), 1367−1370. (m) van der Boom, M. E.; Liou, S.-Y.; Shimon, L. J. W.; Ben-David, Y.; Milstein, D. *Inorg. Chim. Acta* **2004**, *357* (13), 4015−4023. (n) Castonguay, A.; Beauchamp, A. L.; Zargarian, D. *Inorg. Chem.* **2009**, *48* (7), 3177−3184.

(6) (a) Gómez-Benítez, V.; Baldovino-Pantaleón, O.; Herrera-Álvarez, C.; Toscano, R. A.; Morales-Morales, D. *Tetrahedron Lett.* **2006**, *47* (29), 5059−5062. (b) Vabre, B.; Lindeperg, F.; Zargarian, D. *Green Chem.* **2013**, *15* (11), 3188−3194. (c) Vabre, B.; Petiot, P.; Declercq, R.; Zargarian, D. *Organometallics* **2014**, *33* (19), 5173−5184. (d) Estudiante-Negrete, F.; Hernández-Ortega, S.; Morales-Morales, D. *Inorg. Chim. Acta* **2012**, *387*, 58−63. (e) Chakraborty, S.; Krause, J. A.; Guan, H. *Organometallics* **2009**, *28* (2), 582−586. (f) Zhang, J.; Medley, C. M.; Krause, J. A.; Guan, H. *Organometallics* **2010**, *29* (23), 6393−6401. (g) Chakraborty, S.; Patel, Y. J.; Krause, J. A.; Guan, H. *Polyhedron* **2012**, *32* (1), 30−34.

(7) (a) Pandarus, V.; Zargarian, D. *Chem. Commun.* **2007**, *9*, 978−980. (b) Hao, J.; Vabre, B.; Mougang-Soume, B.; Zargarian, D. *Chem. - Eur. J.* **2014**, *20* (39), 12544−12552. (c) Hao, J.; Mougang-Soume, B.; Vabre, B.; Zargarian, D. *Angew. Chem., Int. Ed.* **2014**, *53* (12), 3218−3222. (d) Pandarus, V.; Castonguay, A.; Zargarian, D. *Dalton Trans.* **2008**, *35*, 4756−4761.

(8) (a) Spasyuk, D. M.; Zargarian, D.; van der Est, A. *Organometallics* **2009**, *28* (22), 6531−6540. (b) Spasyuk, D. M.; Zargarian, D. *Inorg. Chem.* **2010**, *49* (13), 6203−6213. (c) Zhang, B.-S.; Wang, W.; Shao, D.-D.; Hao, X.-Q.; Gong, J.-F.; Song, M.-P. *Organometallics* **2010**, *29* (11), 2579−2587. (d) Niu, J.-L.; Chen, Q.-T.; Hao, X.-Q.; Zhao, Q.-X.; Gong, J.-F.; Song, M.-P. *Organometallics* **2010**, *29* (9), 2148−2156. (e) Spasyuk, D. M.; Gorelsky, S. I.; van der Est, A.; Zargarian, D. *Inorg. Chem.* **2011**, *50* (6), 2661−2674. (f) Yang, M.-J.; Liu, Y.-J.; Gong, J.-F.; Song, M.-P. *Organometallics* **2011**, *30* (14), 3793−3803. (g) Sanford, J.; Dent, C.; Masuda, J. D.; Xia, A. *Polyhedron* **2011**, *30* (6), 1091−1094.

(9) (a) Fan, L.; Foxman, B. M.; Ozerov, O. V. *Organometallics* **2004**, *23* (3), 326−328. (b) Ozerov, O. V.; Guo, C.; Fan, L.; Foxman, B. M. *Organometallics* **2004**, *23* (23), 5573−5580. (c) Liang, L.-C.; Chien, P.-S.; Huang, Y.-L. *J. Am. Chem. Soc.* **2006**, *128* (49), 15562−15563. (d) Liang, L.-C.; Chien, P.-S.; Lin, J.-M.; Huang, M.-H.; Huang, Y.-L.; Liao, J.-H. *Organometallics* **2006**, *25* (6), 1399−1411. (e) Adhikari, D.; Huffman, J. C.; Mindiola, D. J. *Chem. Commun.* **2007**, *43*, 4489−4491. (f) Adhikari, D.; Pink, M.; Mindiola, D. J. *Organometallics* **2009**, *28* (7), 2072−2077. (g) Fryzuk, M. D.; Montgomery, C. D. *Coord. Chem. Rev.* **1989**, *95*, 1. (h) Ingleson, M. J.; Fullmer, B. C.; Buschhorn, D. T.;

DOI: 10.1021/acs.organomet.5b00272
Organometallics 2015, 34, 3520−3531

Fan, H.; Pink, M.; Huffman, J. C.; Caulton, K. G. *Inorg. Chem.* **2008**, *47* (2), 407−409. (i) Fryzuk, M. D.; MacNeil, P. A. *J. Am. Chem. Soc.* **1981**, *103* (12), 3592−3593.
(10) (a) Vechorkin, O.; Proust, V.; Hu, X. *J. Am. Chem. Soc.* **2009**, *131* (28), 9756−9766. (b) Madhira, V. N.; Ren, P.; Vechorkin, O.; Hu, X.; Vicic, D. A. *Dalton Trans.* **2012**, *41*, 7915. (c) Breitenfeld, J.; Scopelliti, R.; Hu, X. *Organometallics* **2012**, *31* (6), 2128−2136.
(11) Vabre, B.; Canac, Y.; Duhayon, C.; Chauvin, R.; Zargarian, D. *Chem. Commun.* **2012**, *48* (84), 10446−10448.
(12) (a) Zargarian, D.; Castonguay, A.; Spasyuk, D., ECE-Type Pincer Complexes of Nickel. In *Topics in Organometallic Chemistry*; van Koten, G.; Milstein, D., Eds.; Springer: Berlin, 2013; Vol. *40*, pp 131−173. (b) Wang, Z.-X.; Liu, N. *Eur. J. Inorg. Chem.* **2012**, *2012* (6), 901−911.
(13) Pandarus, V.; Zargarian, D. *Organometallics* **2007**, *26* (17), 4321−4334.
(14) (a) Chakraborty, S.; Zhang, J.; Krause, J. A.; Guan, H. *J. Am. Chem. Soc.* **2010**, *132* (26), 8872−8873. (b) Salah, A. B.; Offenstein, C.; Zargarian, D. *Organometallics* **2011**, *30* (20), 5352−5364. (c) Castonguay, A.; Spasyuk, D. M.; Madern, N.; Beauchamp, A. L.; Zargarian, D. *Organometallics* **2009**, *28* (7), 2134−2141. (d) Knapen, J. W. J.; van der Made, A. W.; de Wilde, J. C.; van Leeuwen, P. W. N. M.; Wijkens, P.; Grove, D. M.; van Koten, G. *Nature* **1994**, *372* (6507), 659−663.
(15) (a) Vabre, B.; Spasyuk, D. M.; Zargarian, D. *Organometallics* **2012**, *31* (24), 8561−8570. (b) Vabre, B.; Lambert, M. L.; Petit, A.; Ess, D. H.; Zargarian, D. *Organometallics* **2012**, *31* (17), 6041−6053. (c) Salah, A. B.; Zargarian, D. *Dalton Trans.* **2011**, *40* (35), 8977−8985.
(16) (a) Choi, J.; MacArthur, A. H. R.; Brookhart, M.; Goldman, A. S. *Chem. Rev.* **2011**, *111* (3), 1761−1779. (b) Zhu, K.; Achord, P. D.; Zhang, X.; Krogh-Jespersen, K.; Goldman, A. S. *J. Am. Chem. Soc.* **2004**, *126* (40), 13044−13053. (c) Krogh-Jespersen, K.; Czerw, M.; Zhu, K.; Singh, B.; Kanzelberger, M.; Darji, N.; Achord, P. D.; Renkema, K. B.; Goldman, A. S. *J. Am. Chem. Soc.* **2002**, *124* (36), 10797−10809. (d) Göttker-Schnetmann, I.; White, P.; Brookhart, M. *J. Am. Chem. Soc.* **2004**, *126* (6), 1804−1811. (e) Roddick, D. M. *Topics in Organometallic Chemistry*; 2013; Vol. *40* (Organometallic Pincer Chemistry), pp 49−88.
(17) Lefèvre, X.; Durieux, G.; Lesturgez, S.; Zargarian, D. *J. Mol. Catal. A: Chem.* **2011**, *335* (1−2), 1−7.
(18) Pratt, D. A.; Pesavento, R. P.; van der Donk, W. A. *Org. Lett.* **2005**, *7* (13), 2735−2738.
(19) Based on two CCDC surveys, both conducted on November 4, 2014, of all structurally characterized nickel compounds containing a covalently bonded triflate anion and of all complexes bearing at least one Ni-N≡CR moiety.
(20) It has been shown that the presence of *t*-Bu substituents *ortho* to the phosphinite moieties in (POCOP)NiBr generates significantly shorter P−Ni bond distances. See ref 15a.
(21) (a) Chakraborty, S.; Patel, Y. J.; Krause, J. A.; Guan, H. *Angew. Chem., Int. Ed.* **2013**, *52* (29), 7523−7526. (b) Lefevre, X.; Spasyuk, D. M.; Zargarian, D. *J. Organomet. Chem.* **2011**, *696* (4), 864−870.
(22) Liang, S.; Wang, H.; Deb, T.; Petersen, J. L.; Yee, G. T.; Jensen, M. P. *Inorg. Chem.* **2012**, *51* (23), 12707−12719.
(23) Rozenel, S. S.; Kerr, J. B.; Arnold, J. *Dalton Trans.* **2011**, *40* (40), 10397−10405.
(24) The relative ν(C≡N) values observed in these adducts is also reflected in the greater electrophilicity of the double-bond moiety in the acrylonitrile adduct of **1** in regard to its aliphatic counterpart (see Table 2).
(25) It should be noted that this comparison was based on ν(C≡N) values measured under identical experimental conditions, i.e., using KBr disks for the comparison between [(H-POCOP^{Ph})Ni(NCMe)][OSO$_2$CF$_3$] and **1**, and using solid samples in ATR-IR to compare **1** to **9**.
(26) Note: Both of these signals are fairly broad, LW$_{1/2}$ being ∼118 Hz for the new signal at ca. 193−194 ppm and 115 Hz for the cationic adduct **8** signal at ca. 195 ppm.
(27) Grove, D. M.; van Koten, G.; Ubbels, H. J. C.; Zoet, R.; Spek, A. L. *Organometallics* **1984**, *3* (7), 1003−1009.
(28) To better understand the curious formation of the triflate derivatives (NCN)Ni(OTf) and (PC$_{sp3}$P$^{i\text{-}Pr}$)Ni(OTf) in non-negligible amounts, we set out to establish if they arise from the corresponding acetonitrile adducts bearing triflate counter-anions. The following experiment was conducted for this purpose: to a 0.04 or 0.08 mM C_6D_6 solution of complex **1** was added 1−10 equiv of silver triflate, the sample was agitated periodically, and the ^{31}P NMR spectra were recorded after 24 h. The original signal broadened slightly, but there was no trace of the triflate derivative (singlet at 185 ppm) or any other new species. This led us to believe that there might indeed be an equilibrium where the triflate moiety would exchange with the acetonitrile ligand, albeit shifted much more to the acetonitrile adduct.
(29) Foti, M. C.; Daquino, C.; Mackie, I. D.; DiLabio, G. A.; Ingold, K. U. *J. Org. Chem.* **2008**, *73*, 9270−9282.

DOI: 10.1021/acs.organomet.5b00272
Organometallics 2015, 34, 3520−3531